Sonodynamic Therapy

Literature Seminar

2018. 12. 13

Kazuki Takahashi (M1)

Index

1. Introduction
   - About ultrasound
   - Various medical uses of ultrasound
   - Safety range of frequency and intensity

2. Sonodynamic therapy for cancer cells
   - Photodynamic therapy & sonodynamic therapy
   - Example of drugs used for sonodynamic therapy
   - Mechanism & Drug design

Index

1. Introduction
   - About ultrasound
   - Various medical uses of ultrasound
   - Safety range of frequency and intensity

2. Sonodynamic therapy for cancer cells
   - Photodynamic therapy & sonodynamic therapy
   - Example of drugs used for sonodynamic therapy
   - Mechanism & Drug design

About ultrasound

- Ultrasound

  - a mechanical wave through the displacements of the molecules constituting the medium in which the wave is travelling.
  - similar in character to audible sound, but at frequencies greater than 20 kHz.
  - a fundamentally different wave phenomenon from electromagnetic waves such as radio waves, infrared radiation and X-rays.

Various medical uses of ultrasound

- Diagnosis

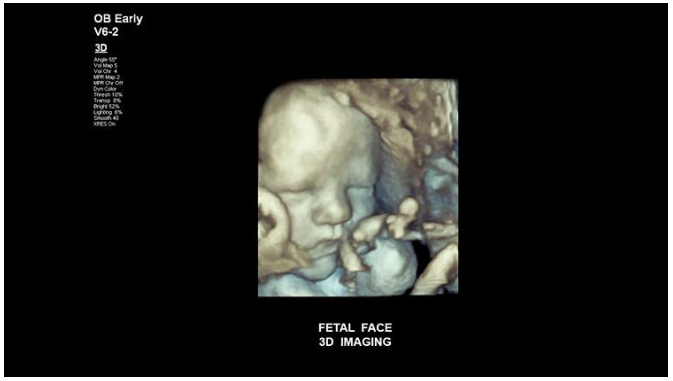

https://www.philips.co.jp/healthcare/product/HC795200/epiq-7-ultrasound-machine#galleryTab=CLI

- Lithotripsy

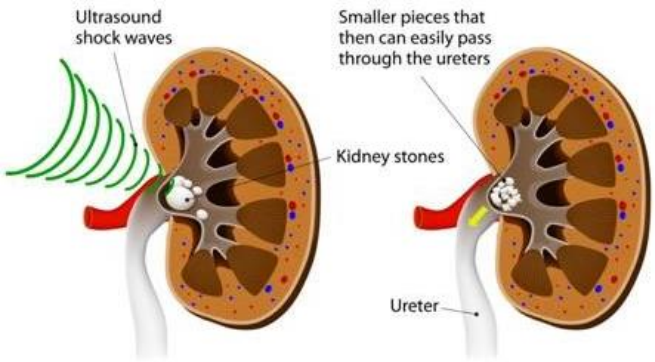

https://www.practo.com/health-wiki/lithotripsy-meaning-procedure-and-cost/134/article

- Fracture healing

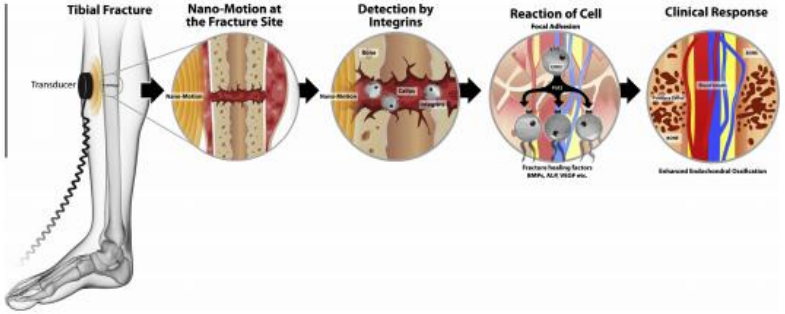

A. Harrison, *et al., Ultrasonics*, **2016**, *70*, 45

- HIFU (High-intensity focused ultrasound)

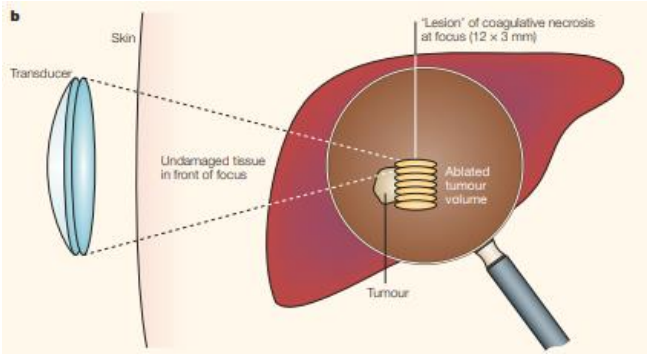

James E. K, *Nat. Rev. Cancer*, **2005**, *5*, 321

Practical range of frequency

- In the frequency range between 1 MHz and 20 MHz
  - practical use in clinical medicine for diagnostic, therapeutic and destructive purposes.

- The attenuation of the ultrasonic energy depends on the frequency of the wave.
  - the average attenuation coefficient in soft tissue
    $=0.5\ dB\ cm^{-1}\ MHz^{-1}$

Gail ter Haar, *The Safe Use of Ultrasound in Medical Diagnosis 3rd Edition*, 2012, p9

- 5 MHz: 80% loss within the first 2.8 cm of tissue.
- 3 MHz: 80% loss within the first 4.7 cm of tissue.
- 2 MHz: 80% loss within the first 7.0 cm of tissue.
- 1 MHz: 80% loss within the first 14 cm of tissue.

The treatments by US are available within the first 10 cm of tissue.

X. Qian, *et al.*, *Adv. Mater.*, **2016**, *28*, 8097

US intensity

表2　その他の超音波医療機器

機器の種類	周波数	強度
診断用（体内構造のイメージング）		
・エコーカディオグラフィ（心エコー）	5MHz	3.4mW/cm²
・エコーセファグラフィ（脳エコー）	5MHz	3.4mW/cm²
・ドプラー血流計	5~10MHz	150mW/cm²
・産科用診断装置	2.25MHz	6.3mW/cm²
手術用（熱及び機械的作用による組織の破壊）		
・胆石の破砕	0.1MHz	20~100W/cm²
治療用（温熱あるいは非温熱作用）		
・物理療法及びリハビリテーション	0.75~3MHz	0.1~5W/cm²

- High intensity of US makes burn and cell death.
- Low intensity is not effective.
- US intensity is recommended between 0.1~5 MHz for treatment.

W/cm

Atsumi Ohota, *理学療法の歩み*, **2006**, *17*, 14

Hydroxyl radical produced by cavitation

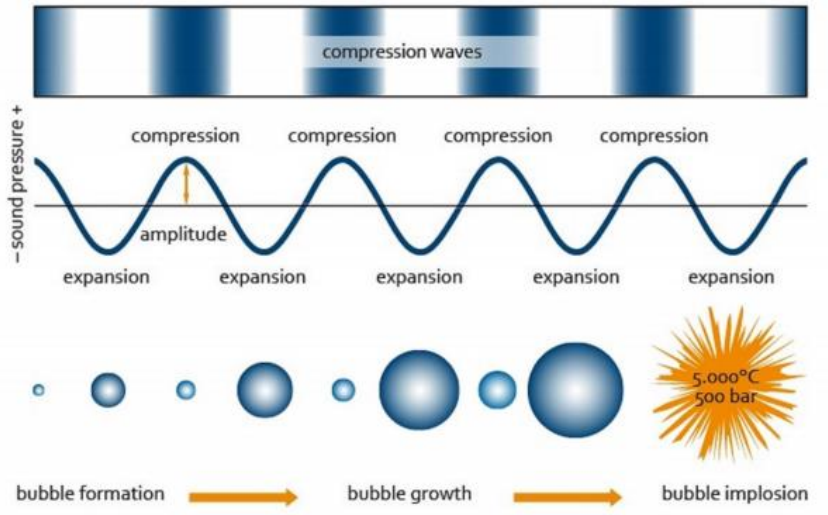

Figure 1. Principle of ultrasound cavitation [16]. The initiated bubbles grow due to evaporation and finally reach critical size (resonant) when it grows quickly and collapse violently.

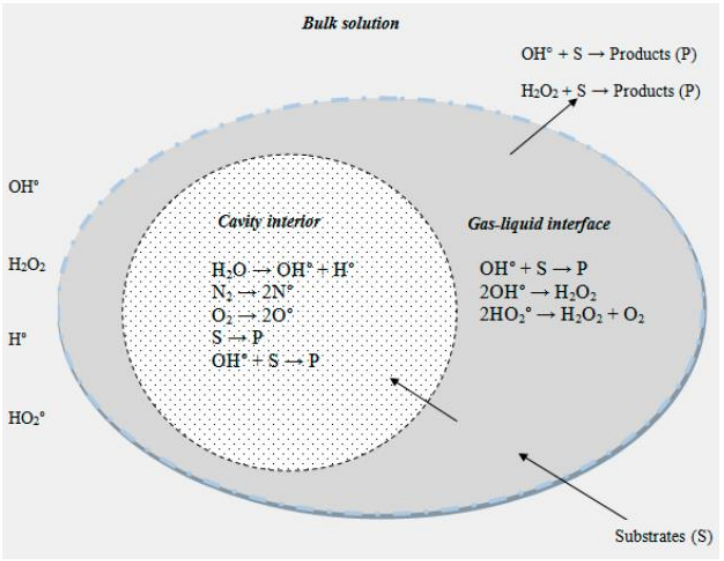

Figure 1. The reaction zone in the cavitation process (adapted from Chowdhury et al., 2009).

- Ultrasonic irradiation of liquids causes acoustic cavitations, i.e., the formation, growth and implosive collapse of bubbles.
- Such cavitation generates local sites of high temperature and pressure for short periods of time.
- The extreme temperature conditions generated by a collapsing bubble can also lead to the formation of radical chemical species.

Örjan J., *et al., Sustainable and energy efficient leaching of tungsten (W) by ultrasound controlled cavitation*, **2018**, p8

Sabina Z., *et al.*, *Proceedings*, **2018**, *2*, 188

Sonoluminescence produced by cavitation

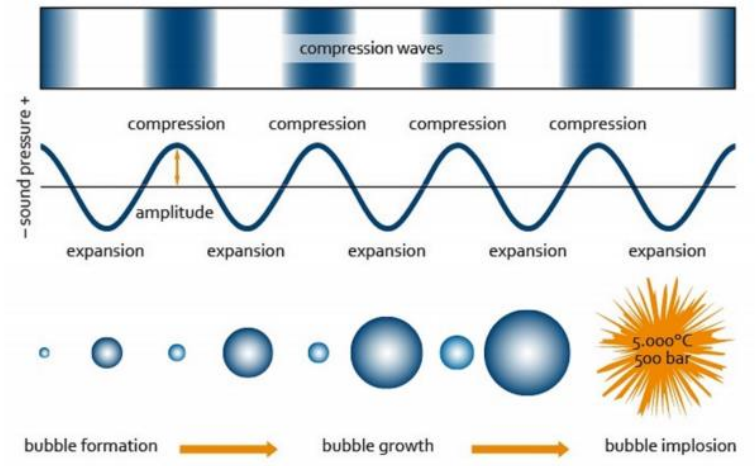

Figure 1. Principle of ultrasound cavitation [16]. The initiated bubbles grow due to evaporation and finally reach critical size (resonant) when it grows quickly and collapse violently.

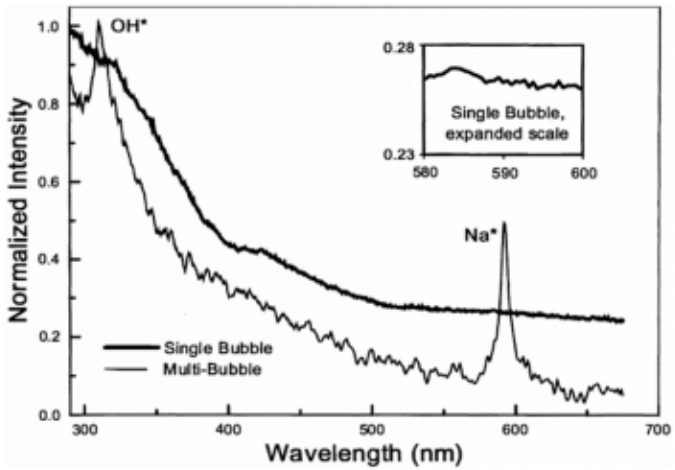

Figure 4 Multi-Bubble and Single-Bubble Sonoluminescence background subtracted spectra in 0.1 M NaCl solutions in water. Curves are not to scale and are standardised to the maximum intensity of each = 1.0. As well as a 'continuous' component, the Multi-Bubble graph shows clearly two identifiable peaks, at 310 nm, corresponding to OH* and at around 590 nm corresponding to Na*. The SBSL graph only shows a regular 'continuous' or 'featureless' pattern. Reproduced from[79] Matula T, Roy R, Mourad P, McNamara W, Suslick KS. Comparison of Multibubble and Single-Bubble Sonoluminescence Spectra. Phys. Rev. Letters 1995; 75(13):2602–2605 (with permission)

- The high temperatures generated in the collapsing bubbles by the increasing pressure would make the heated gases in the bubbles emit light.
- The spectrum of MBSL in water shows peaks that correspond to excited state OH* (mainly at 310 nm)

Örjan J., *et al., Sustainable and energy efficient leaching of tungsten (W) by ultrasound controlled cavitation*, **2018**, p8

Franc¸ois Hibou, *Homeopathy*, **2017**, *106*, 181

Short summary

- US is used for Diagnosis, Fracture healing, Lithotripsy, HIFU, and so on.
- US is able to penetrate into deep tissues (ten centimeter).
- Around 1 MHz of US frequency is recommended for practical use into deep tissues .
- 0.1~5 W/cm^2 of US intensity is also recommended.
- Cavitation in water generates hydroxy radical and other radical species, and makes sonoluminescence.

Index

1. Introduction
   - About ultrasound
   - Various medical uses of ultrasound
   - Safety range of frequency and intensity

2. Sonodynamic therapy for cancer cells
   - Photodynamic therapy & sonodynamic therapy
   - Example of drugs used for sonodynamic therapy
   - Mechanism & Drug design

Photodynamic therapy (PDT)

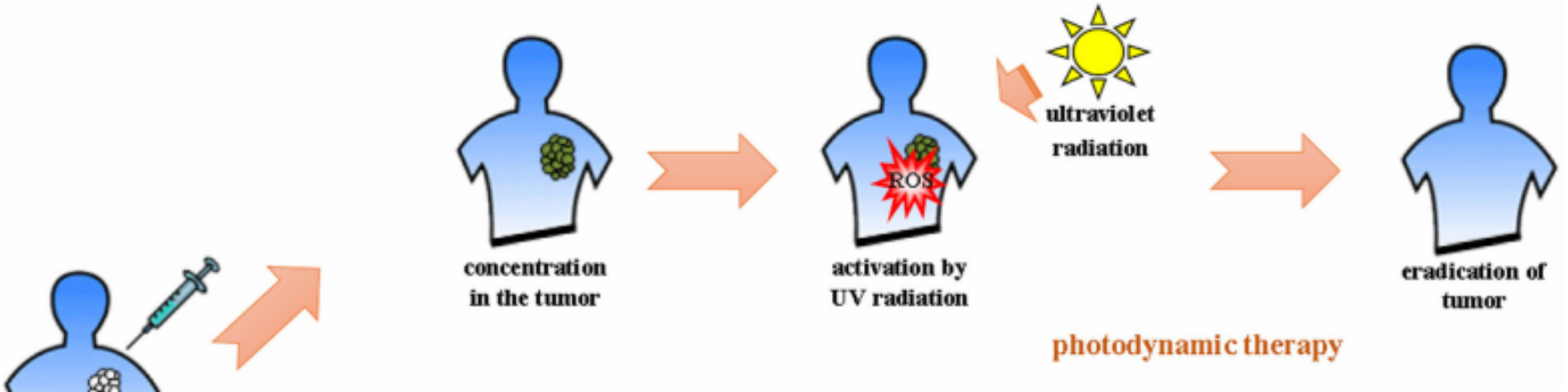

- Side-effects are more suppressed.
- PDT is not used for tumors in the deep place of the body.

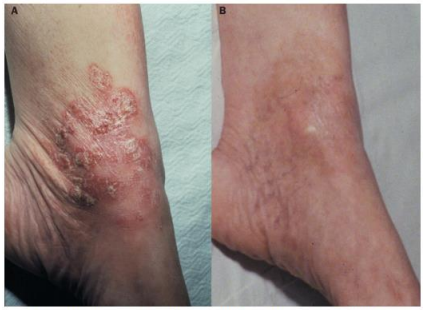

Figure 2. Patient with Bowen's disease before treatment with aminolevulinic acid PDT (A), and 2 months after treatment (B). The single treatment was shown by histological analysis to have irradicated the lesion, which did not recur. The excellent healing after treatment is apparent.

Stanley B. B., *et al.*, *Lancet Oncol.*, **2004**, *5*, 497

Fig. 2 Milestones of photodynamic therapy (PDT) and sonodynamic therapy (SDT) in tumor treatment. Cancer therapies, such as PDT or SDT, build on the administration of sensitive agents into tumor, followed by their activation by UV radiation or US wave, respectively. Activated photo- or sonosensitizers generate ROS that lead to cancer cell eradication

Bogdan, *et al., Nanoscale Res. Lett.*, **2017**, *12*, 225

Photodynamic Therapy (PDT)

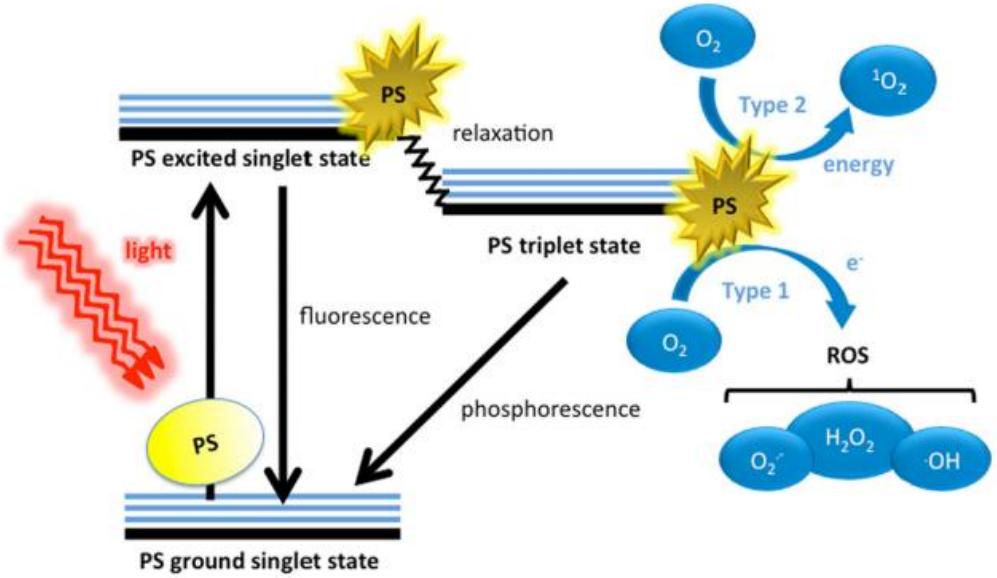

FIGURE 1 | Schematic illustration of photodynamic therapy including the Jablonski diagram. The PS initially absorbs a photon that excites it to the first excited singlet state and this can relax to the more long lived triplet state. This triplet PS can interact with molecular oxygen in two pathways, type I and type II, leading to the formation of reactive oxygen species (ROS) and singlet oxygen respectively.

Tianhong D., *et al.*, *Front. Microbiol.*, **2012**, *3*, 120

ROS produced by photosensitizer & light has cytotoxicity.

Basic chemical structures for PDT

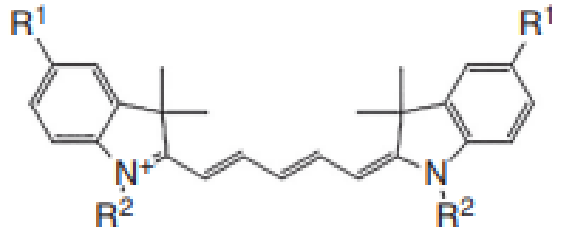

Cyanine

Abs_{max} (nm): >700
$Emis_{max}$ (nm): >800

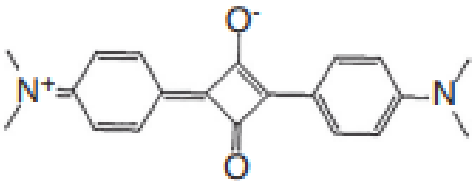

Squaraine

Abs_{max} (nm): 650–800
$Emis_{max}$ (nm): >800

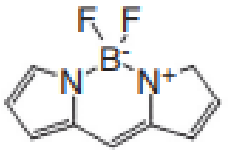

BODIPY

Abs_{max} (nm): 650–800
$Emis_{max}$ (nm): >700

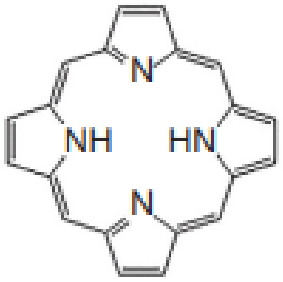

Porphyrin

Abs_{max} (nm): 650–800
$Emis_{max}$ (nm): 700–1000

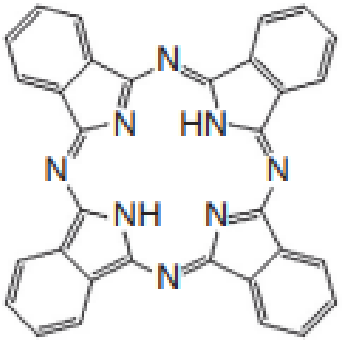

Phthalocyanine

Abs_{max} (nm): 650–800
$Emis_{max}$ (nm): 700–1000

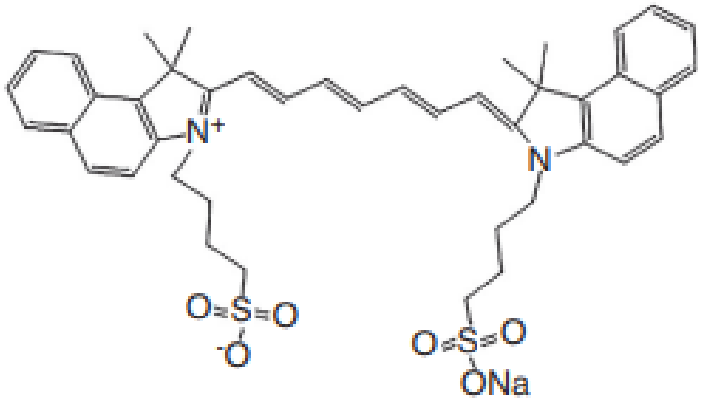

Indocyanine green

Abs_{max} (nm): 788
$Emis_{max}$ (nm): 813

Ankit, S. *et al. Drug Discovery Today.* **2018**, *23*, 5

Sonodynamic therapy (SDT)

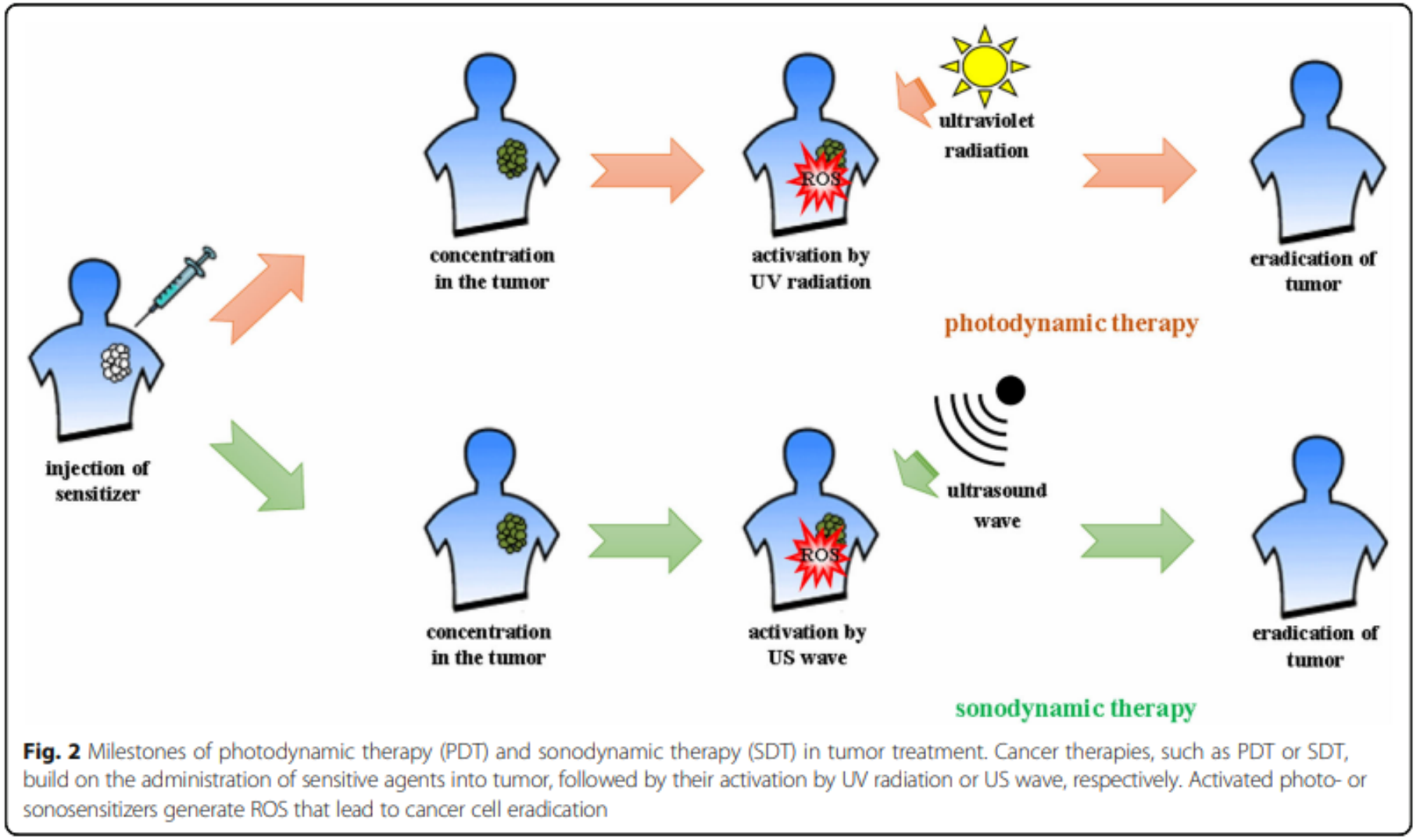

Fig. 2 Milestones of photodynamic therapy (PDT) and sonodynamic therapy (SDT) in tumor treatment. Cancer therapies, such as PDT or SDT, build on the administration of sensitive agents into tumor, followed by their activation by UV radiation or US wave, respectively. Activated photo- or sonosensitizers generate ROS that lead to cancer cell eradication

Bogdan, *et al., Nanoscale Res. Lett.*, **2017**, *12*, 225

Sonodynamic therapy (SDT)

- Deeper penetration
- Non-invasive treatment
- Good repeatability

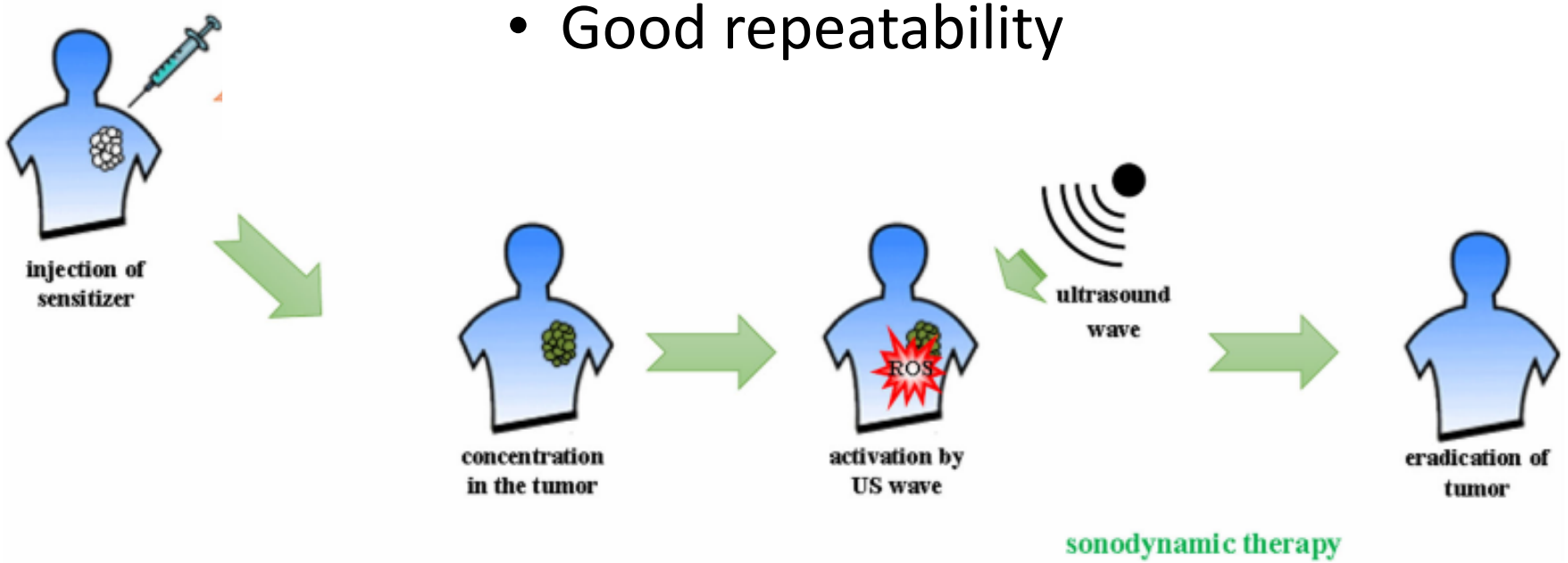

Fig. 2 Milestones of photodynamic therapy (PDT) and sonodynamic therapy (SDT) in tumor treatment. Cancer therapies, such as PDT or SDT, build on the administration of sensitive agents into tumor, followed by their activation by UV radiation or US wave, respectively. Activated photo- or sonosensitizers generate ROS that lead to cancer cell eradication

Bogdan, *et al., Nanoscale Res. Lett.*, **2017**, *12*, 225

First example of drugs used for SDT

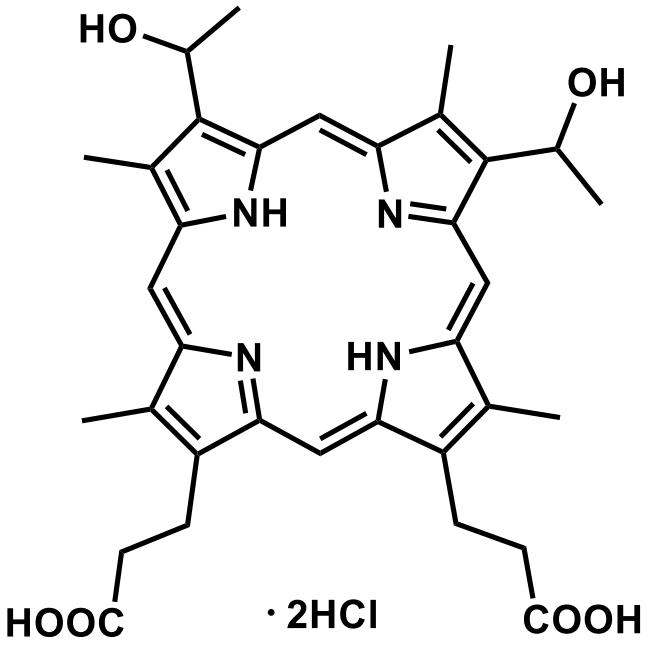

Hematoporphyrin dihydrochloride

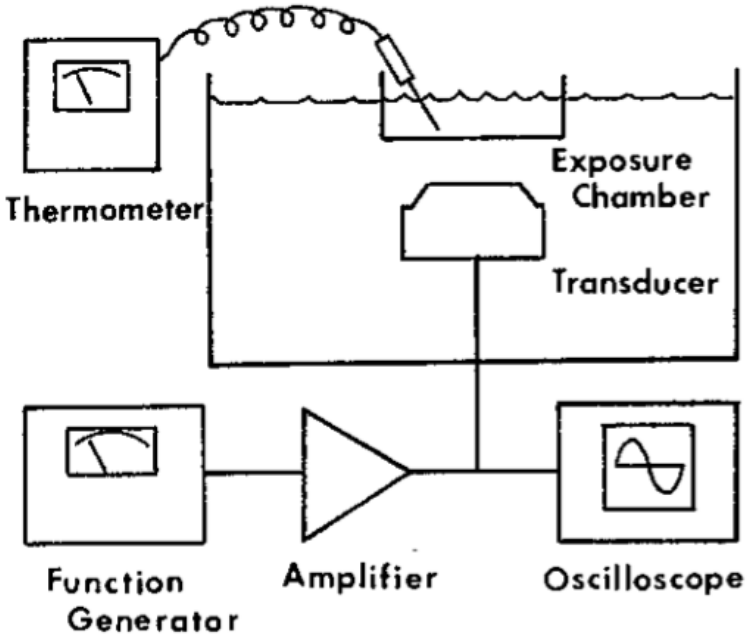

Fig. 1. Schematic diagram of the US irradiation system.

Yumita, N *et al.*, *Jpn. J. Cancer Res.*, **1989**, *80*, 219

First example of drugs used for SDT

Table I. Unstained Fraction after Exposure to US for 60 Seconds

Tumor line	Intensity (W/cm^2)	Hp conc. ($\mu g/ml$)	N[a]	Unstained fraction	P[b]
Sarcoma 180	1.27	0	3	0.843±0.019	
		50	3	0.335±0.035	*P*
	2.21	0	3	0.292±0.133	
		50	3	0.172±0.100	
	3.18	0	4	0.215±0.102	
		10	4	0.140±0.094	
		25	4	0.024±0.020	*P*
		50	4	0.023±0.004	*P*
AH 130	1.27	0	3	0.833±0.019	
		50	3	0.779±0.028	
	2.21	0	3	0.253±0.031	
		50	3	0.054±0.003	*P*
	3.18	0	3	0.142±0.017	
		10	3	0.089±0.007	*P*
		25	3	0.047±0.010	*P*
		50	3	0.045±0.012	*P*

a) Number of experiments.
b) Significantly different from the value of US alone at the same intensity.

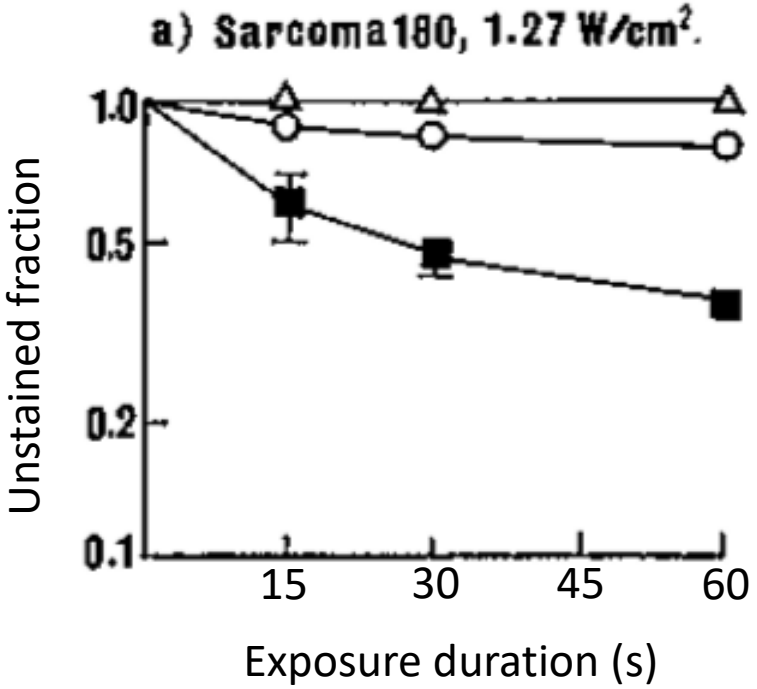

△: 50 mg/mL Hp alone
○: US alone
■: 50 mg/mL Hp + US

Yumita, N *et al.*, *Jpn. J. Cancer Res.*, **1989**, *80*, 219

Other examples of drugs used for SDT

Porphyrin compound sensitizers

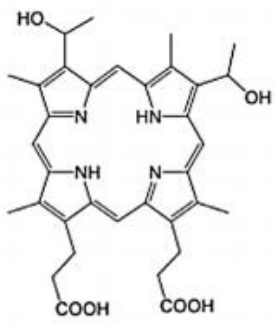

Hematoporphyrin

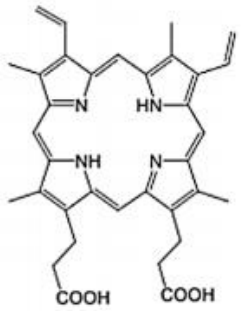

$R^1, R^2 = OCH_3$, OH or OH, OCH_3
Hematoporphyrin monomethyl ether

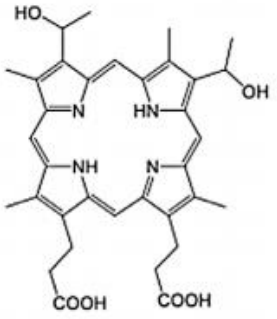

Protoporphyrin IX

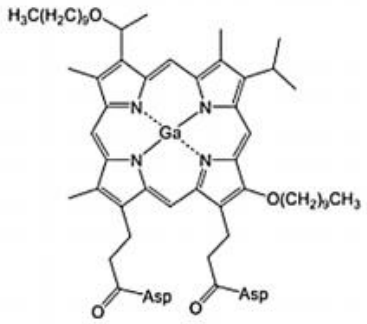

ATX-70

Xanthone compound sensitizers

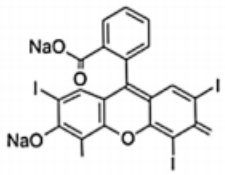

Erythosin B (EB)

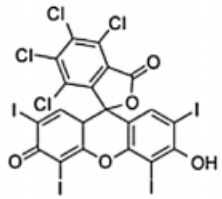

Rose bengal (RB)

non-steroid anti-inflammatory agent sensitizers

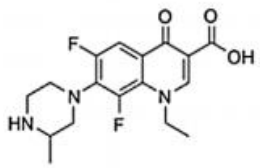

Lomefloxacin (LFLX)

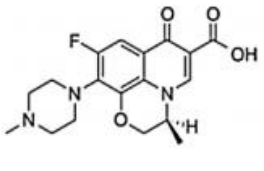

Levofloxacin (LVFX)

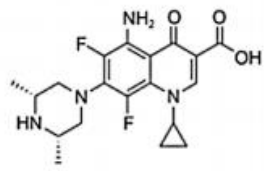

Sparfloxacin (SPFX)

Other sound-sensitizers

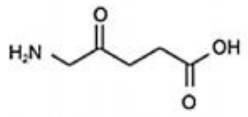

5-aminolevulinic acid (5-ALA)

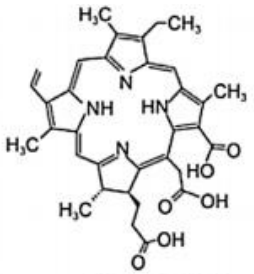

Chlorin e6 (Ce6)

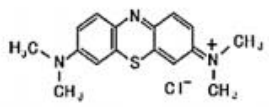

Methylene blue

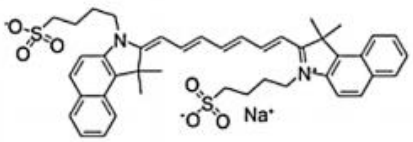

Indocyanine green (ICG)

Liu R., *et al.*, *Photodiagnosis and Photodynamic Therapy*, **2017**, *19*, 159

Mechanism of SDT (*in vitro*)

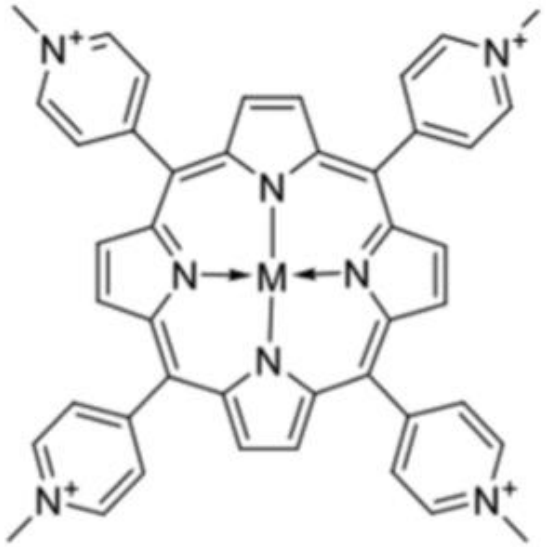

1: M = $2H^+$ **2**: M = $Fe^{3+}(Cl)$

3: M = Zn^{2+} **4**: M = Pd^{2+}

Fig. 1. Structures of porphyrins 1–4.

- Investigating the US-responsiveness of a variety of metal-porphyrin complexes, freebase porphyrin and Fe(III), Zn(II) and Pd(II) porphyrin.
- Analyzing their ROS generation under US exposure and related bio-effects.

F. Giuntini, *et al., Free Radical Biology and Medicine,* **2018**, *121*, 190

Sono-induced ROS detected by EPR

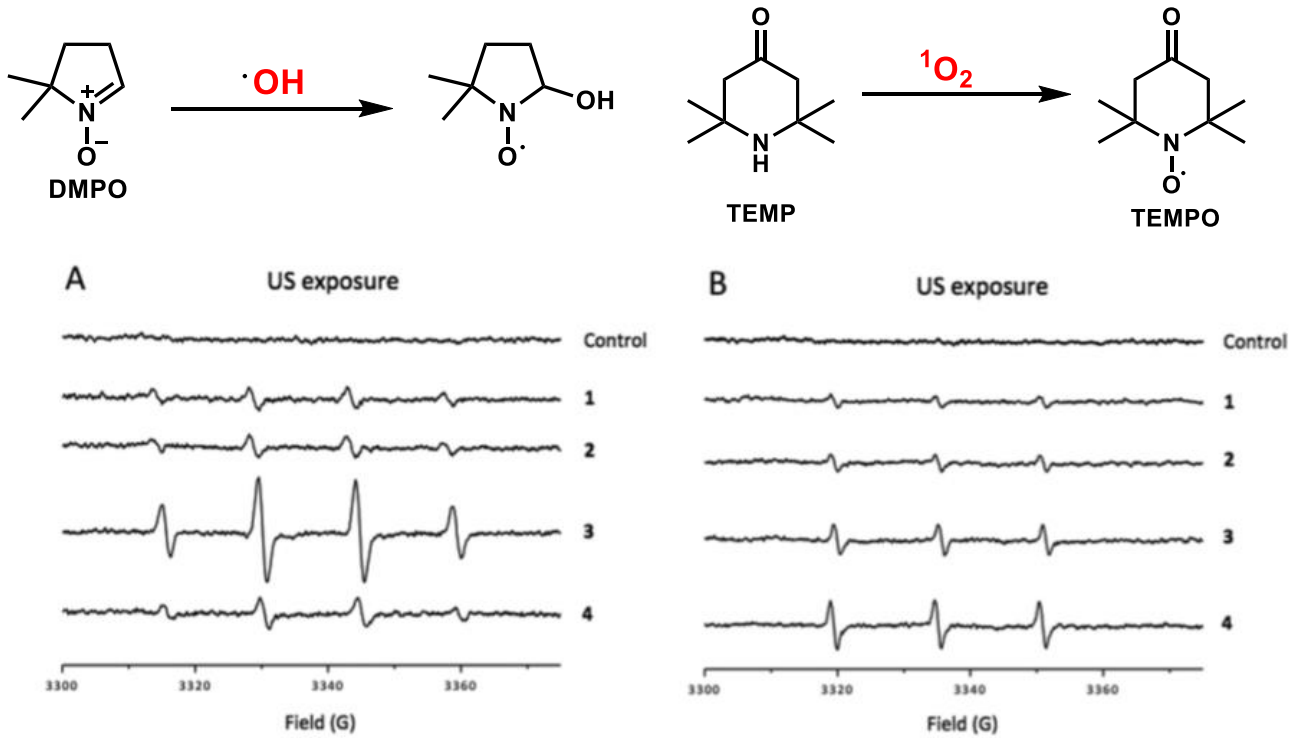

Fig. 2. Generation of hydroxyl radicals (A) and of singlet oxygen (B) by the various porphyrins (**1–4**) following activation by US power at 1.5 W/cm^2 for 5 min at 1.866 MHz, as detected by EPR spectroscopy. Signal intensity is proportional to the amount of reactive species generated.

- Porphyrin 3 has the highest hydroxyl radical generation efficiency.
- Porphyrin 4 generated most singlet oxygens.

F. Giuntini, *et al., Free Radical Biology and Medicine,* **2018**, *121*, 190

Sonoluminescence

- Sonoluminescence emission spectra

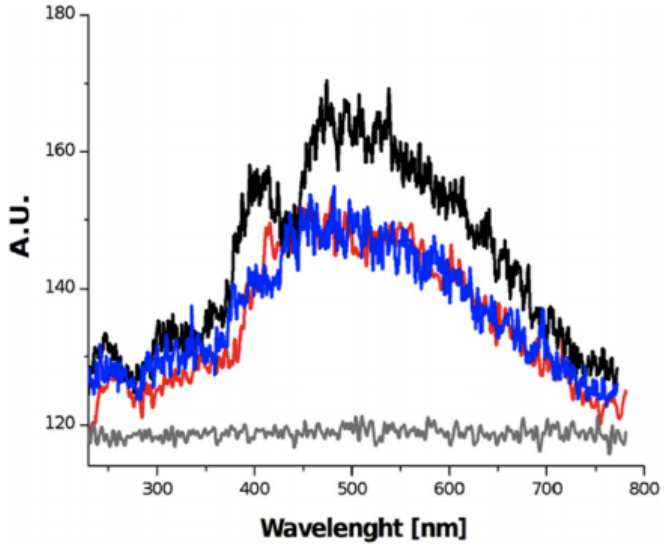

Fig. 4. Sonoluminescence emission spectra of porphyrin **3** (black curve) and **4** (red curve) solutions under air saturation during US irradiation at 1.5 W/cm^2 for 5 min, at 1.866 MHz. The blue curve refers to multi bubble sonoluminescence (MBSL) recorded in aqueous solution, while the grey curve corresponds to the background of the acquiring system.

- SL emitted both in water (blue) and in the presence of porphyrins 3 (**black**) and 4 (red).
- The hydroxyl radical emission observed in the presence of porphyrin 3.

F. Giuntini, *et al., Free Radical Biology and Medicine,* **2018**, *121*, 190

Effects of SDT on HT-29 cells

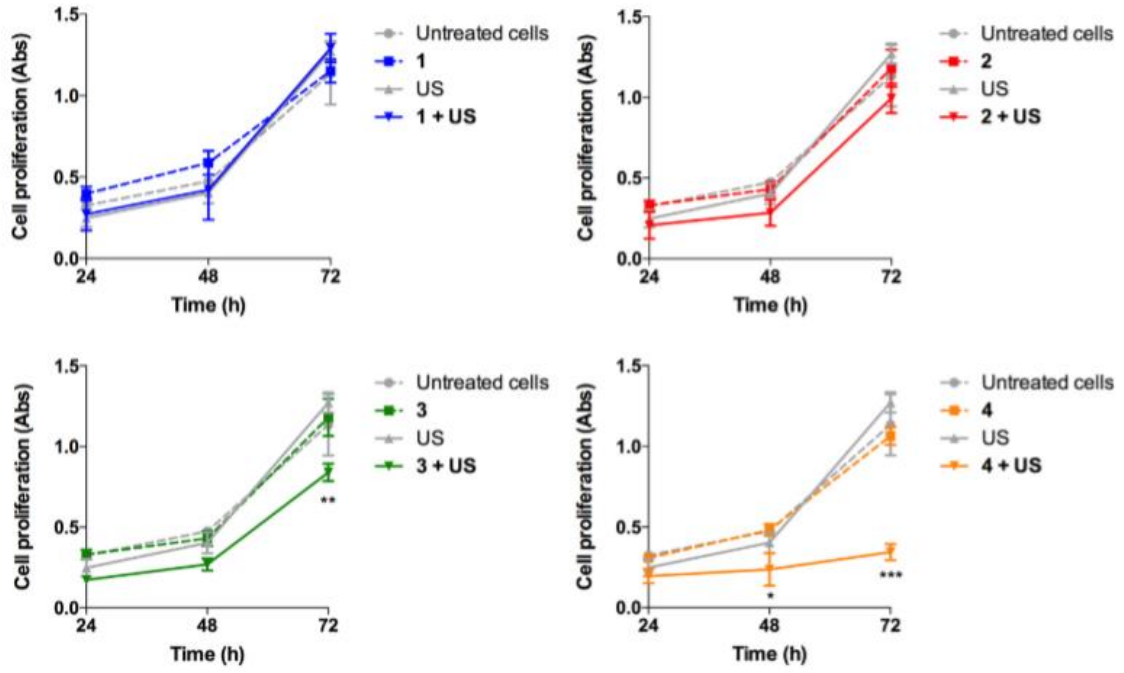

Fig. 6. Effects of sonodynamic treatment on HT-29 cell growth. HT-29 cells were incubated for 24 h with the various porphyrins (1, 2 and 4 at 500 µM; 3 at 250 µM) and then exposed to US power at 1.5 W/cm^2 for 5 min at 1.866 MHz. Cell proliferation was evaluated after 24, 48 and 72 h using the WST-1 assay. Statistically significant difference *versus* untreated cells: * $p < 0.05$, ** $p < 0.01$.

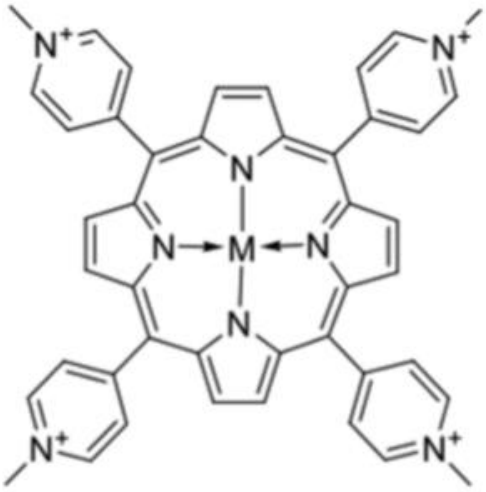

Fig. 1. Structures of porphyrins 1–4.

- Porphyrin 1 and 2 did not cause a significant reduction in HT-29 cell growth under US exposure.
- porphyrin 3 and 4 lead to a significant HT-29 cell growth decrease under US exposure.

F. Giuntini, *et al., Free Radical Biology and Medicine,* **2018**, *121*, 190

Cell death analysis

Table 1
Cell death analysis 24 h after treatment.

HT-29 cells	Live cells	Apoptotic cells	Necrotic cells
Untreated cells	95.2 ± 8.3	2.5 ± 0.9	2.3 ± 0.6
Light	94.9 ± 9.2	4.1 ± 1.0	0.9 ± 0.2
US	95.0 ± 7.3	3.2 ± 0.7	1.8 ± 0.5
4	95.4 ± 8.4	4.0 ± 0.6	0.6 ± 0.1
4 + Light	53.3 ± 4.5***	7.0 ± 0.9	39.7 ± 2.5***
4 + US	60.4 ± 5.8***	19.9 ± 3.1**	19.7 ± 4.5**

Statistical significance *vs* untreated cells: .
** $p < 0.01$.
*** $p < 0.001$.

Detected by Dead Cell Apoptosis Kit, with Annexin V-Alexa Fluor® and propidium iodide.

- 4 + US induced both necrotic and apoptotic cell death.
- Light exposure was responsible for necrotic cell death because the higher singlet oxygen production.

F. Giuntini, *et al., Free Radical Biology and Medicine,* **2018**, *121*, 190

Cell death by autophagy

- HT-29 cells after SDT with porphyrin **4**

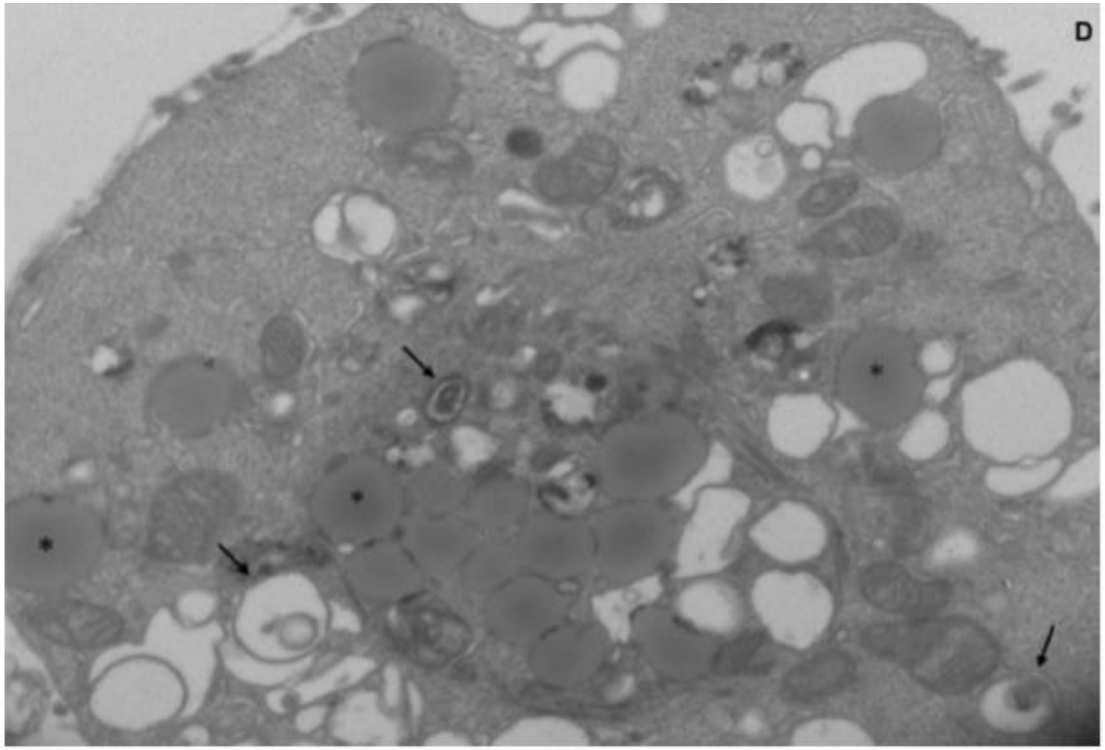

Fig. 10. Representative TEM images of HT-29 cells after sonodynamic treatment with porphyrin **4**. Untreated cells (A, 7500x), cells only exposed to US (1.5 W/cm^2 for 5 min at 1.866 MHz; B, 7500x) and cells 12 h after sonodynamic treatment with porhyrin **4** having been pre-incubated for 24 h at 500 µM (C, 6000x; D, 12,000x) are displayed. Vesicles that contained residual digested material or cellular content are indicated by arrows and lipid droplets by stars.

- Autophagic cell death was observed in this TEM image.

F. Giuntini, *et al., Free Radical Biology and Medicine,* **2018**, *121*, 190

Disscussion

- Metal ions affect the ability of porphyrins to undergo intersystem crossing (ISC) and can also influence the lifetimes of the resulting excited triplets.
- Porphyrin activation by US can be mediated by photo-activation via sonoluminescence.
- SDT of porphyrin 4 is not effective than PDT.

SDT vs PDT

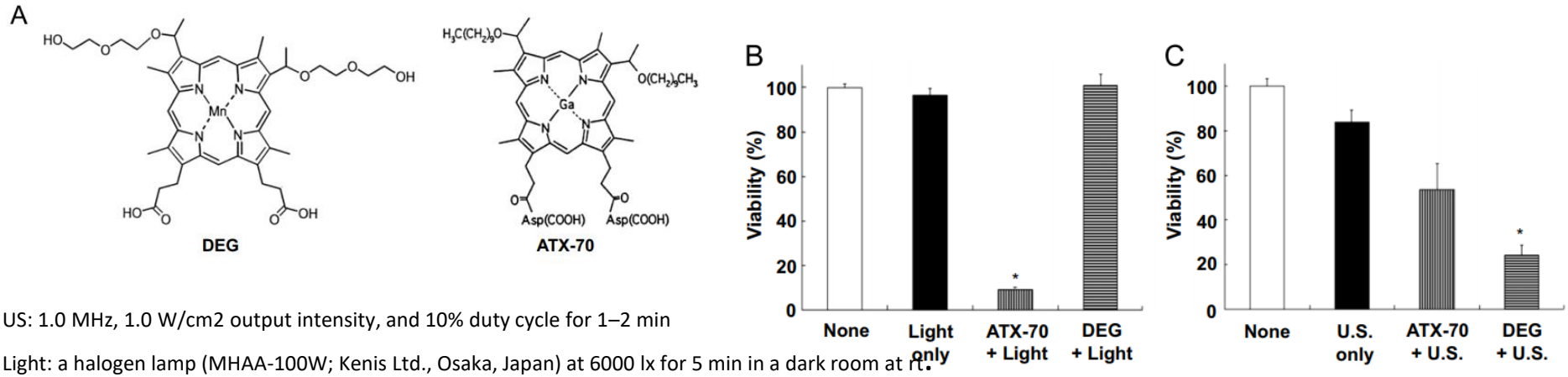

US: 1.0 MHz, 1.0 W/cm2 output intensity, and 10% duty cycle for 1–2 min

Light: a halogen lamp (MHAA-100W; Kenis Ltd., Osaka, Japan) at 6000 lx for 5 min in a dark room at rt.

Fig. 1. Low-intensity ultrasound with DEG results in significant cytotoxicity toward MKN-74 tumor cells. (A) Chemical structures of DEG and ATX-70. (B and C) In vitro phototoxicity and sonotoxicity, respectively, of DEG and ATX-70 for MKN-74 cells. MKN-74 cells suspended in PBS containing 5.0 μM DEG or ATX-70 were exposed to (B) visible light or (C) low-intensity ultrasound, and subsequently cell viability was determined using CCK-8 as described under Materials and methods. None, no treatment; Light/U.S. only, cells were exposed to light or ultrasound only. Data are means ± SD ($n=6$). *$p < 0.001$, significantly different from each other group (Dunnett's test). (D) Fluorescence photomicrographs of cells treated by sonication with or without DEG. Cells were stained using the LIVE/DEAD cell-mediated cytotoxicity kit. Living and dead cells are stained green and red, respectively.

- Exposure to light in the presence of DEG was not cytotoxic for MKN-74 cells, whereas strong phototoxicity was observed with ATX-70.
- MKN-74 cells were significantly damaged by ultrasound irradiation in the presence of DEG, whereas sonotoxicity with ATX-70 was less effective.

H. Tsuru, *et al., Free Radical Biology and Medicine*, **2012**, *53*, 464

Tumor growth analysis

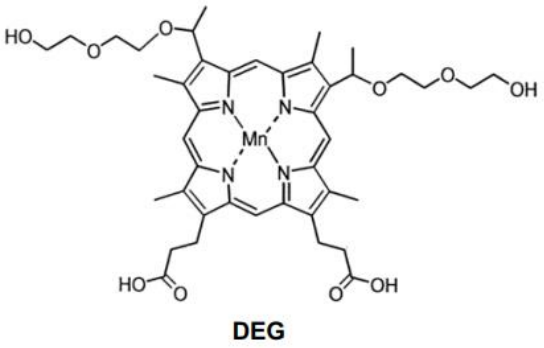

DEG

10 min at 1 MHz, with a 2.0 W/cm^2

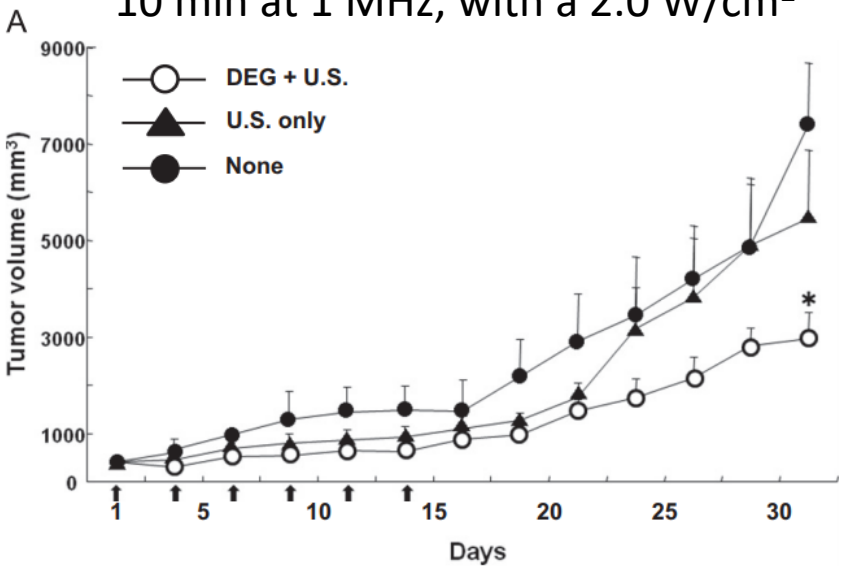

Fig. 4. SDT with DEG greatly inhibits tumor growth in a mouse xenograft model with MKN-74 cells. (A) Antitumor effect of SDT with DEG in a mouse xenograft model. SCID mice were subcutaneously inoculated with 5×10^6 MKN-74 cells. After developing tumors with a diameter of approximately 7 mm, the mice were intravenously injected with DEG and then treated with SDT 10 min later, as described under Materials and methods. Arrows indicate days of treatment with SDT or SDT with DEG. None, no treatment; U.S. only, SDT only; DEG+U.S., SDT with DEG. Data are means ± SD ($n=5$). *$p < 0.05$, significantly different from the no-treatment group (Bonferroni's multiple comparison test). (B) Typical photographs of mice at the end of the experiment, after inoculation with MKN-74 cells and treatment with SDT or SDT with DEG or no treatment.

- SDT with DEG three times a week for 2 weeks potently inhibited tumor growth compared to SDT alone or no treatment.

H. Tsuru*, et al., Free Radical Biology and Medicine*, **2012**, *53*, 464

SDT *in vivo*

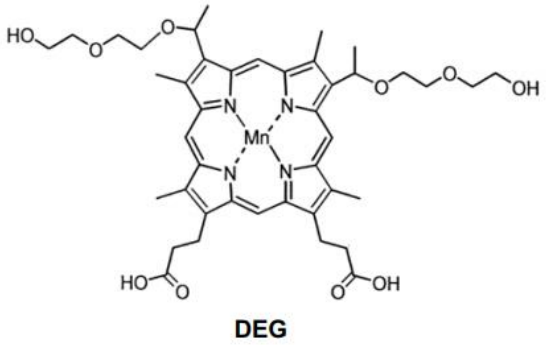

DEG

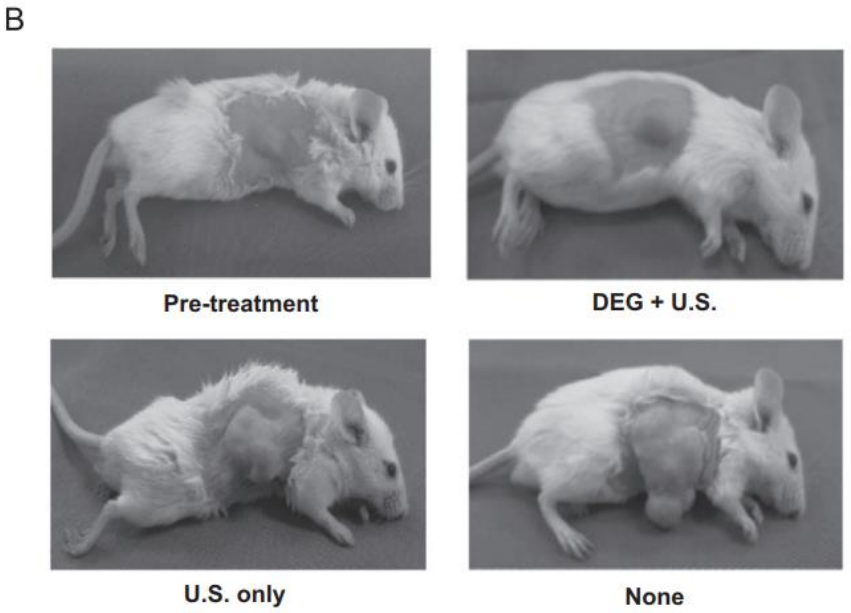

Fig. 4. SDT with DEG greatly inhibits tumor growth in a mouse xenograft model with MKN-74 cells. (A) Antitumor effect of SDT with DEG in a mouse xenograft model. SCID mice were subcutaneously inoculated with 5×10^6 MKN-74 cells. After developing tumors with a diameter of approximately 7 mm, the mice were intravenously injected with DEG and then treated with SDT 10 min later, as described under Materials and methods. Arrows indicate days of treatment with SDT or SDT with DEG. None, no treatment; U.S. only, SDT only; DEG+U.S., SDT with DEG. Data are means ± SD ($n=5$). $^*p < 0.05$, significantly different from the no-treatment group (Bonferroni's multiple comparison test). (B) Typical photographs of mice at the end of the experiment, after inoculation with MKN-74 cells and treatment with SDT or SDT with DEG or no treatment.

- At the end of the experiment, no apparent adverse side effects, including skin sensitivity, were observed in the mice injected with DEG.

H. Tsuru*, et al., Free Radical Biology and Medicine*, **2012**, *53*, 464

Comparative histochemical analysis

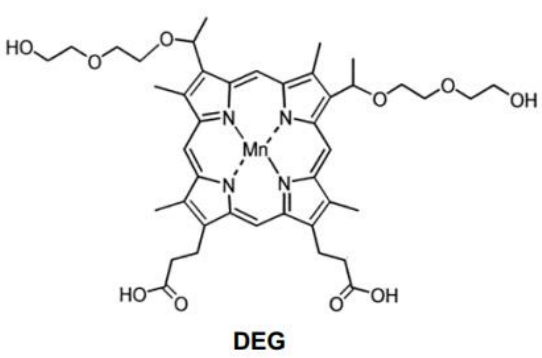

DEG

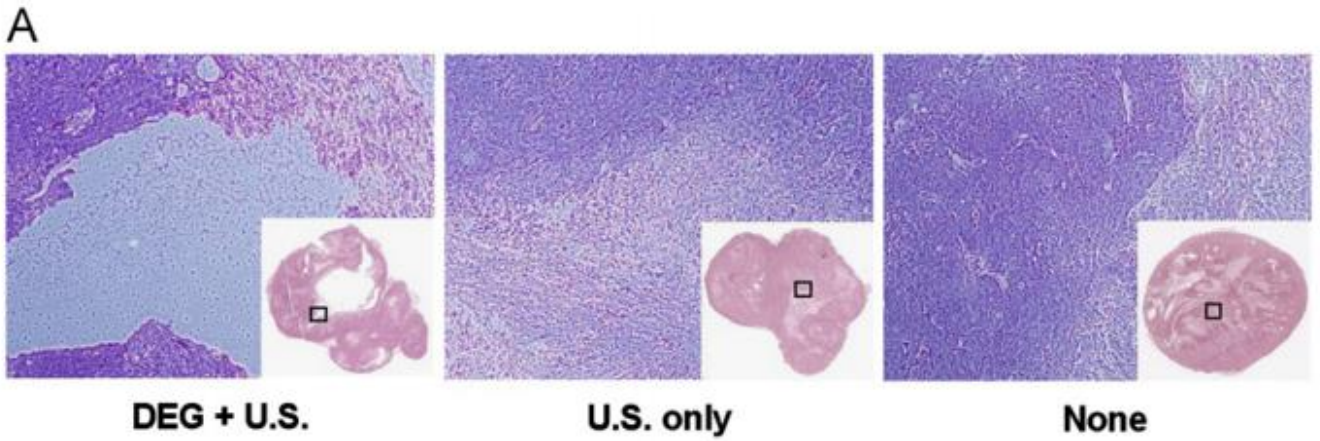

Fig. 5. A large damaged area in the tumor mass after treatment with SDT with DEG. (A and B) Histological sections from the tumors on the final day of treatment with SDT (original magnification 20 ×): (A) H&E staining and (B) ApoMark DNA fragmentation detection kit. Although spontaneous cell damage was detected in all sections with apoptotic cells (dark brown nuclei), a large damaged area (cavity) was observed only in the tumor section that received treatment with U.S.+DEG. Fewer apoptotic cells were detected around the cavity compared to the areas that were spontaneously damaged. At the edge of the cavity in the U.S.+DEG tumor section, apoptotic cells were seldom detected (arrows). The stained cells in the area that was spontaneously damaged seem quite similar in tumor sections from both U.S. only and None.

- spontaneous damage was observed on histochemical analysis in the cancer tissue even without treatment, a large cavity was observed in tumor only after SDT with DEG.

H. Tsuru*, et al., Free Radical Biology and Medicine*, **2012**, *53*, 464

Antibody-drug conjugate (ADC)

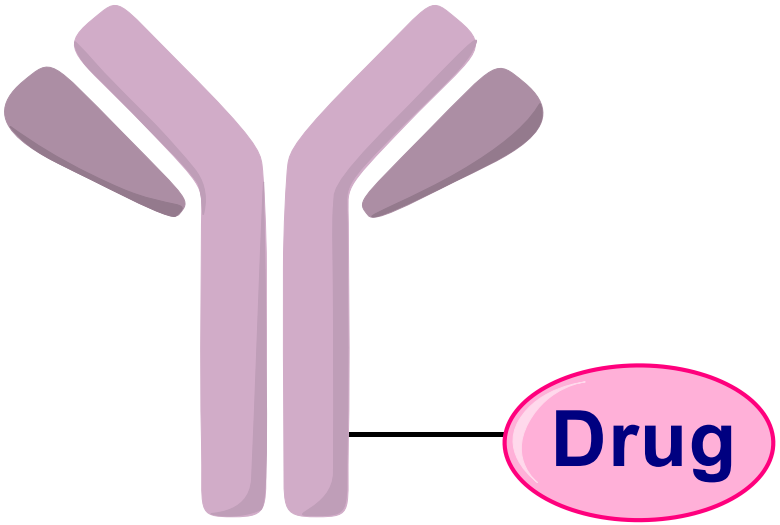

Antibody-drug conjugate (ADC)

- Antibody can carry Drug to the target cells selectively.
- ADC is expected suppressing the side-effect to normal cells.

ADC for Sonodynamic therapy

- How to synthesize ADC (DAR is no data.)

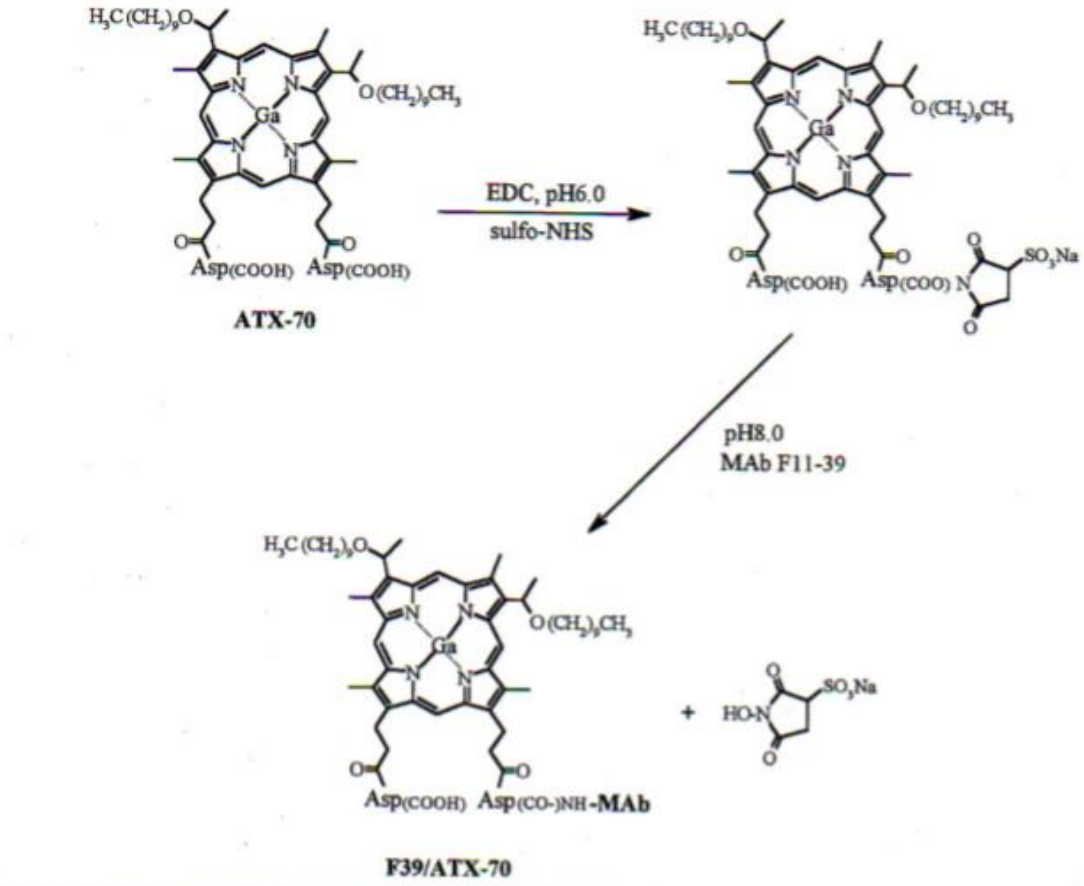

Figure 1. *Schematic representation of preparation of PIC between ATX-70 and F11-39.*

Abe H., *et al.*, *Anticancer Research*, **2002**, *22*, 1575

Example of ADC for SDT

- SDT *in vivo*

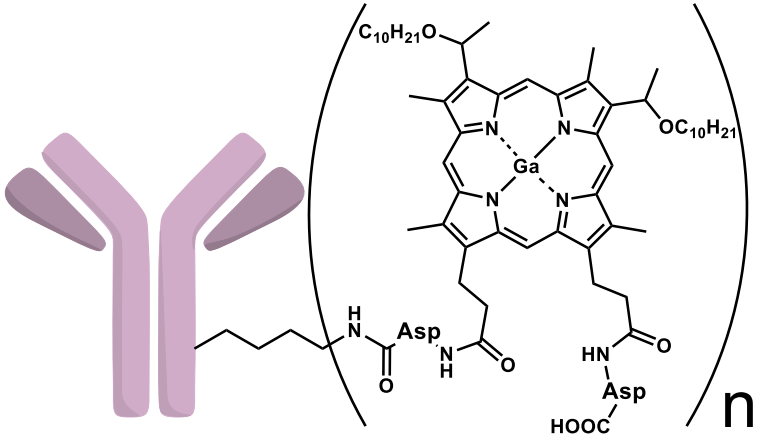

CEA-ATX-70

1 MHz, 2 W/cm^2, 10 min

F39/ATX-70 with US inhibited tumor growth compared to US alone or ATX-70 alone.

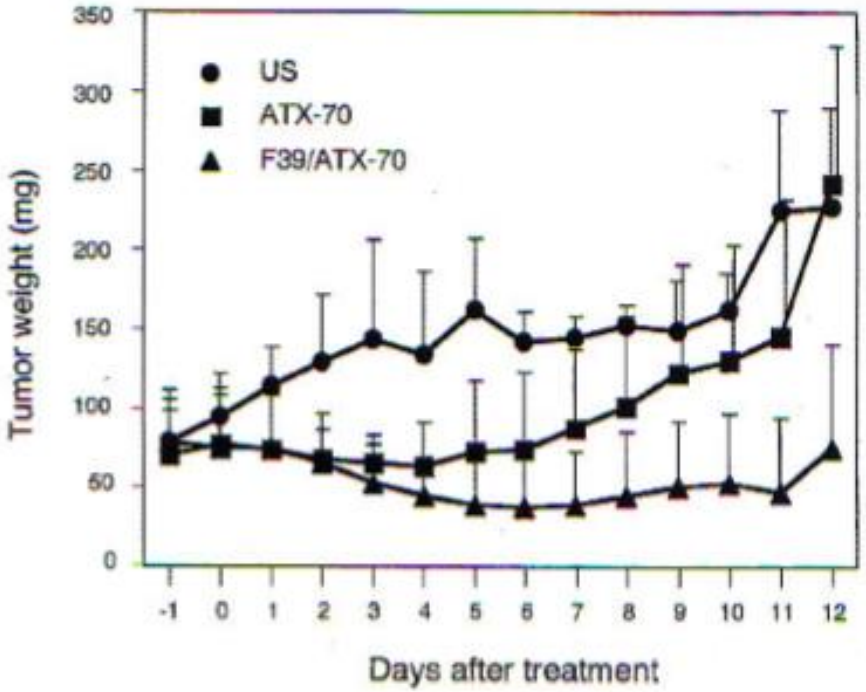

Figure 6. *In vivo antitumor effects of SDT using F39/ATX-70. Balb/c athymic nude mouse were subcutaneously inoculated MKN-45 cells (5 x10^6) on the backs. After development of tumors with a diameter range from 5 to 7 mm, the mice were given intravenous injection of F39/ATX-70 or ATX-70 (3 mg/kg, ATX-70 equivalent) dissolved in PBS (Day -1). After 24 hours (Day 0), the tumor was sonicated with Sonitron 1000. US, ultrasound alone; ATX-70, free ATX-70 plus ultrasound; F39/ATX-70, F39/ATX-70 plus ultrasound. Bars, means ±SD (N=5).*

Abe H., *et al.*, *Anticancer Research*, **2002**, *22*, 1575

Summary

- US frequency is recommended for use around 1 MHz, US intensity is recommended at 1~5 W/cm^2.
- SDT is a non-invasive treatment for tumors located in the deep places of the body.
- Sonosensitizers are activated by sonoluminescence.
- ADC for SDT is few reported, but reported to be effective to tumor.
- SDT and sonochemistry is a developing study, so it will be developed more rapidly in the future.

Appendix

US used at some friquency

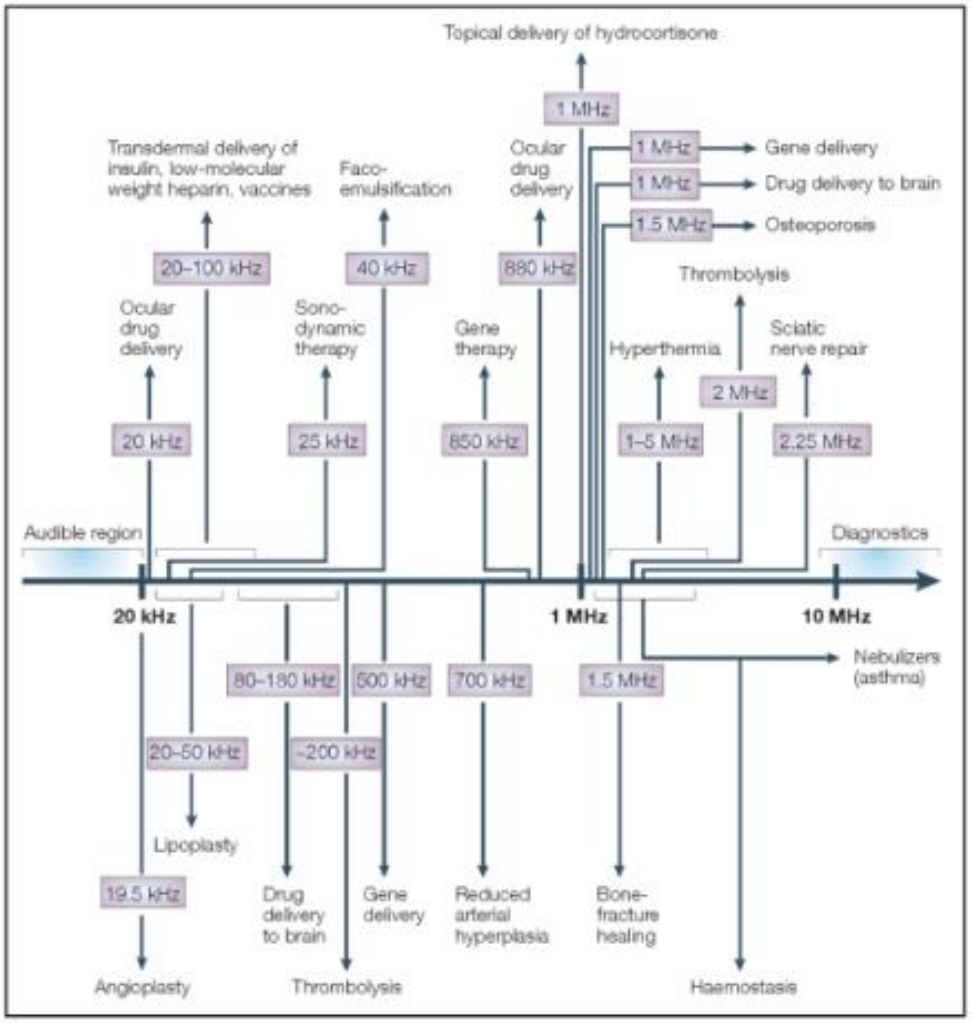

Figure 1. A general summary of biomedical applications of ultrasound at different frequencies, as reported in the literature. Reproduced with permission.[29] Copyright 2005, Nature Publishing Group.

X. Qian*, et al.*, *Adv. Mater.*, **2016**, *28*, 8097

HIFU

- HIFU (High-intensity focused ultrasound)

- Thermal toxicity occurs if tissue temperatures are raised above a threshold of 56° C for at least 1 second, leading to irreversible cell death through coagulative necrosis.

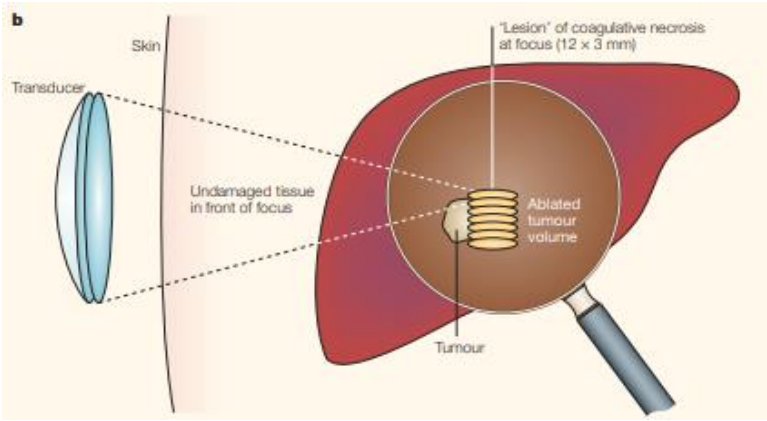

James E. K, *Nat. Rev. Cancer*, **2005**, *5*, 321

Example of ADC for SDT

- SDT *in vivo*

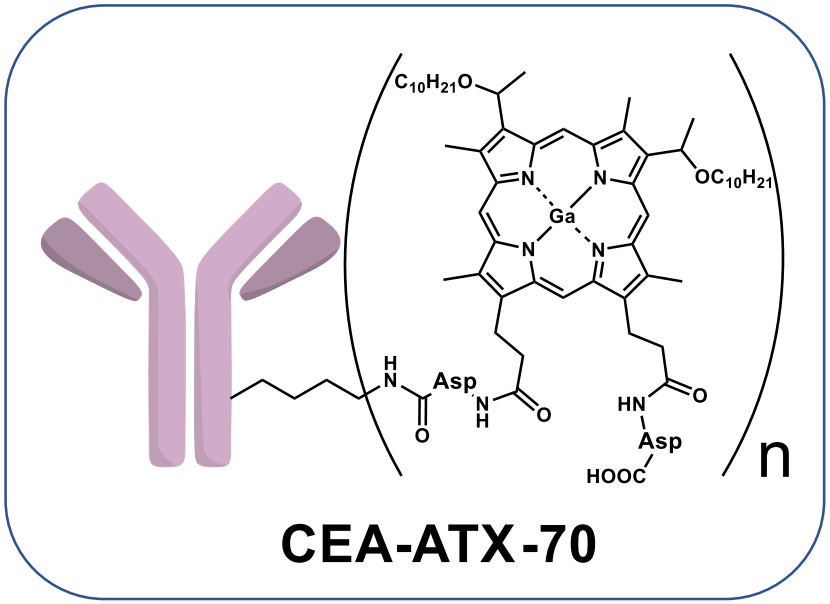

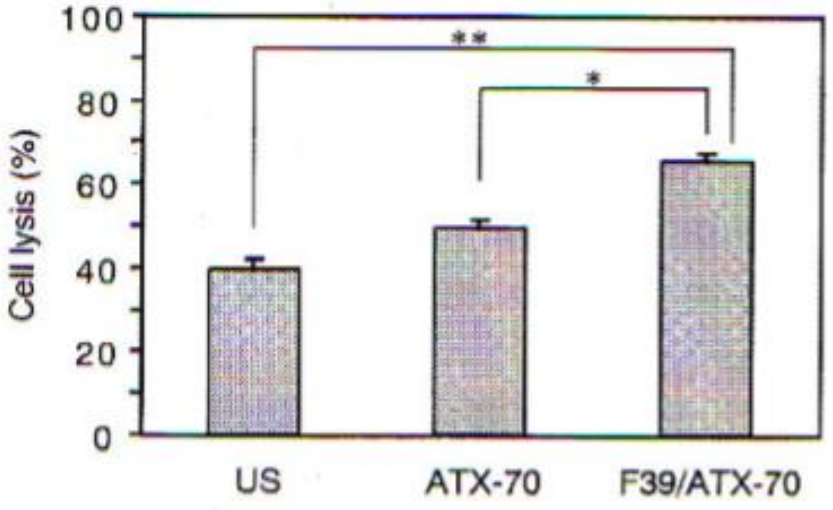

Figure 5. *In vitro sonotoxicity of F39/ATX-70 on CEA-expressing cells. KATO-III cells were incubated with 25 μM ATX-70 or equivalent of F39/ATX-70 in PBS for 1 hour at 4°C. After washing twice, the cells were suspended in 1 ml of air-saturated PBS and given ultrasound. US, ultrasound alone; ATX-70, free ATX-70 plus ultrasound; F39/ATX-70, F39/ATX-70 plus ultrasound. The viability of non-treated cells was 91.5±1.8%. Bars, means±SD (N=5). *, $p < 0.05$; **, $p < 0.01$.*

Abe H., *et al.*, *Anticancer Research*, **2002**, *22*, 1575

SDT in vivo

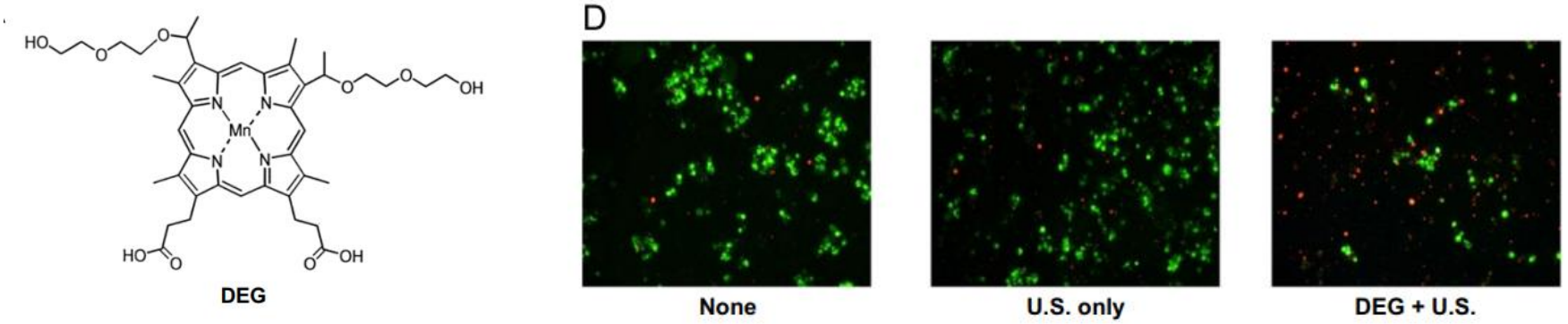

Fig. 1. Low-intensity ultrasound with DEG results in significant cytotoxicity toward MKN-74 tumor cells. (A) Chemical structures of DEG and ATX-70. (B and C) In vitro phototoxicity and sonotoxicity, respectively, of DEG and ATX-70 for MKN-74 cells. MKN-74 cells suspended in PBS containing 5.0 μM DEG or ATX-70 were exposed to (B) visible light or (C) low-intensity ultrasound, and subsequently cell viability was determined using CCK-8 as described under Materials and methods. None, no treatment; Light/U.S. only, cells were exposed to light or ultrasound only. Data are means ± SD ($n=6$). $^*p < 0.001$, significantly different from each other group (Dunnett's test). (D) Fluorescence photomicrographs of cells treated by sonication with or without DEG. Cells were stained using the LIVE/DEAD cell-mediated cytotoxicity kit. Living and dead cells are stained green and red, respectively.

- Visual inspection also showed increased dead cells after ultrasound irradiation with DEG compared to no treatment or the control.

H. Tsuru*, et al., Free Radical Biology and Medicine*, **2012**, *53*, 464

Cell death analysis

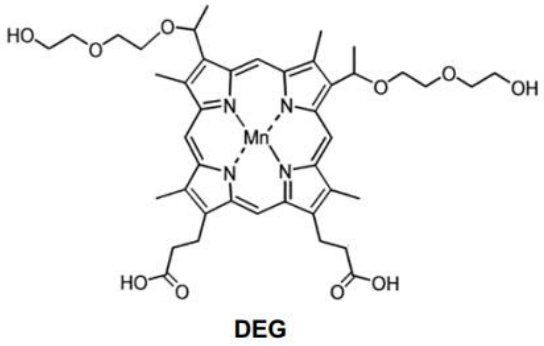

DEG

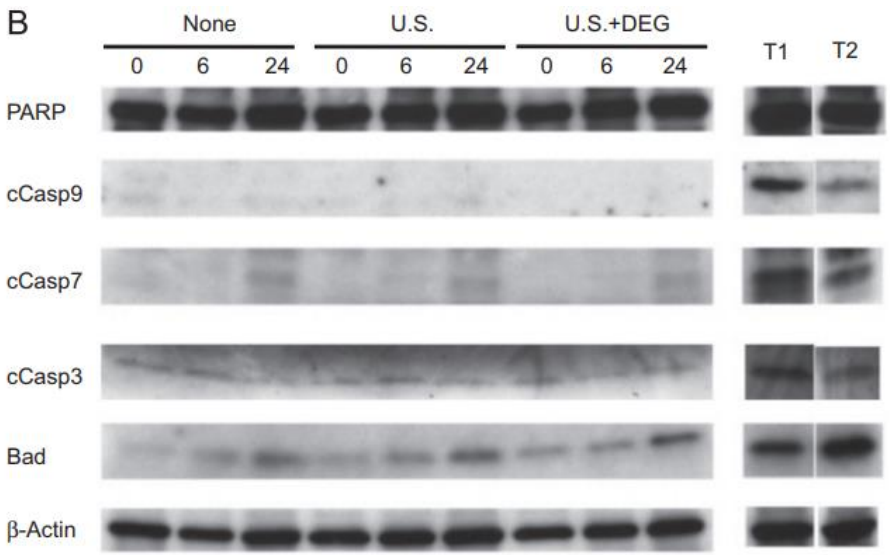

Fig. 2. Sonication with DEG caused damage to MKN-74 cells due to necrosis but not due to apoptosis. (A) No increase in apoptotic cells after sonication with DEG. After exposure to low-intensity ultrasound with or without DEG, MKN-74 cells were analyzed by flow cytometry with the Vybrant Apoptosis Assay Kit No. 8. SYTOX green fluorescence versus R-PE fluorescence was plotted and analyzed using CellQuest Pro software. Although the number of dead cells increased after exposure to ultrasound in the presence of DEG, these were not apoptotic. (B) No apoptotic signals in Western blot analysis after ultrasound irradiation with DEG. Cell lysates were analyzed by Western blotting using antibodies associated with apoptosis. After sonication with or without DEG, no apoptotic signals increased, whereas these signals clearly increased after treating with 0.05% saponin for 2 h (T1) or incubating in PBS for 24 h (T2).

- No apoptotic signals increased after ultrasound irradiation with or without DEG, according to Western blot analysis up to 24 h.

H. Tsuru*, et al., Free Radical Biology and Medicine*, **2012**, *53*, 464

Cell death analysis

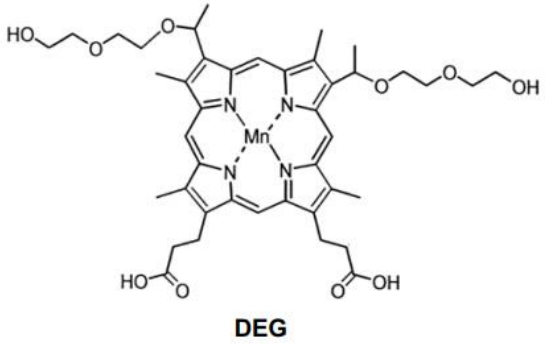

DEG

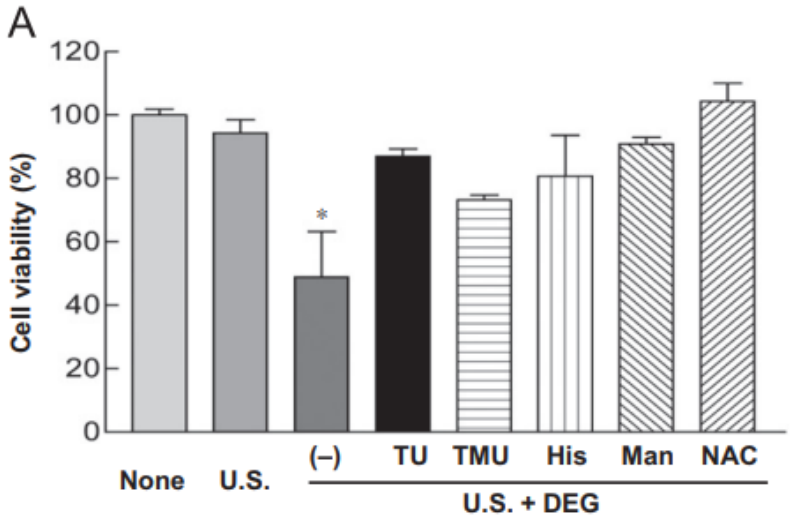

Fig. 3. ROS are generated and mediate sonotoxicity of ultrasound with DEG on MKN-74 cells. (A) ROS were eliminated using ROS scavengers after sonication with DEG. MKN-74 cells in the presence or absence of ROS scavengers (TU and TMU, 10 mM; L-histidine, D-mannitol, or NAC, 0.1 mM) were exposed to low-intensity ultrasound with DEG, and subsequently cell viability was determined using CCK-8 as described under Materials and methods. None, no treatment; U.S., cells were exposed to ultrasound only. Data are means ± SD ($n=6$). $^*p < 0.05$, significantly different from U.S. only group (Dunnett's test). (B) Lipid in the cell membrane became peroxidized after sonication with DEG. Membrane lipid peroxidation of MKN-74 cells was analyzed by flow cytometry using Spy-LHP after sonication with or without DEG. Lipid peroxidation of cell membranes markedly increased after treating with ultrasound with DEG. Plain line with white fill, no treatment; plain line with gray fill, ultrasound irradiation alone; bold line with white fill, sonication with DEG.

H. Tsuru*, et al., Free Radical Biology and Medicine*, **2012**, *53*, 464

Photo-induced ROS detected by EPR

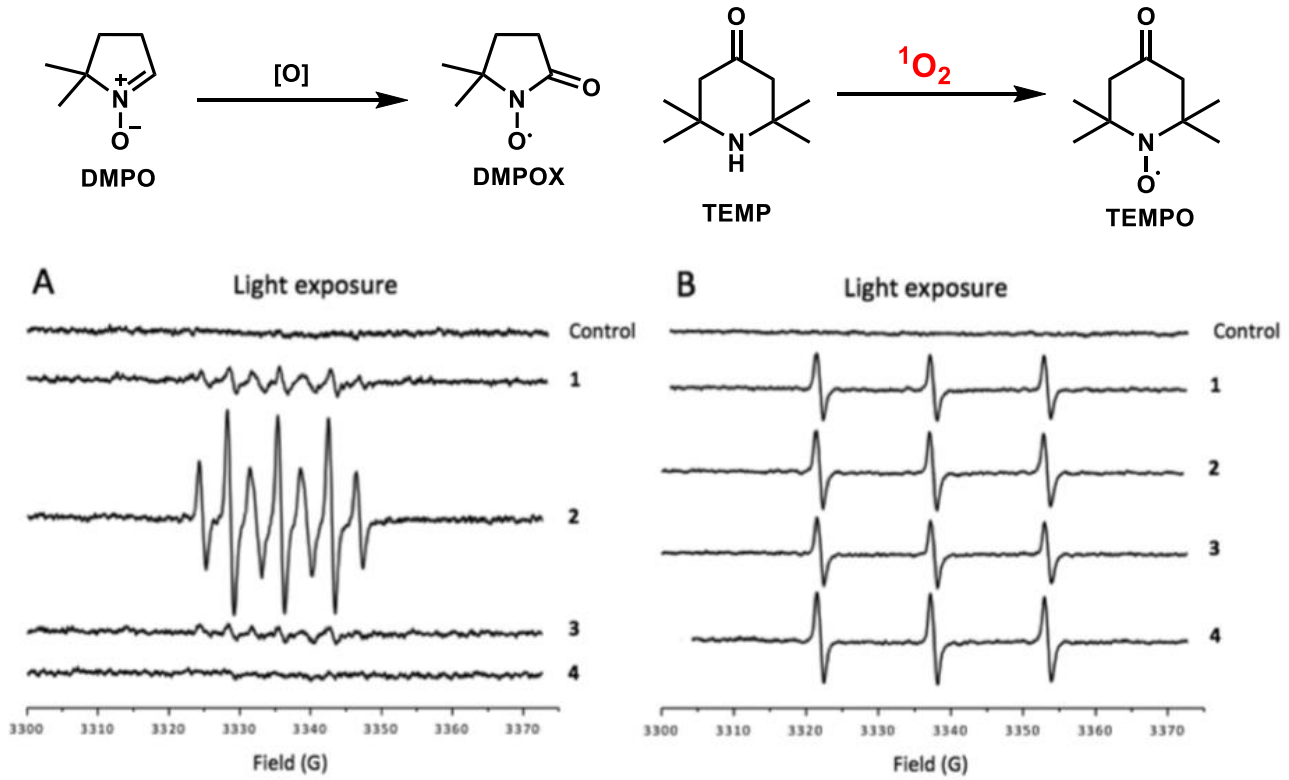

Fig. 3. Generation of hydroxyl radicals (A) and of singlet oxygen (B) by the various porphyrins (1–4) following activation by light power at 51.8 mW/cm^2 for 5 min at 400–1050 nm, as detected by EPR spectroscopy. Signal intensity is proportional to the amount of reactive species generated.

- All porphyrins showed comparable singlet oxygen generation efficiency.
- Light irradiation is more efficient than US exposure for excitation.

F. Giuntini, *et al., Free Radical Biology and Medicine,* **2018**, *121*, 190

Oxidation of DMPO

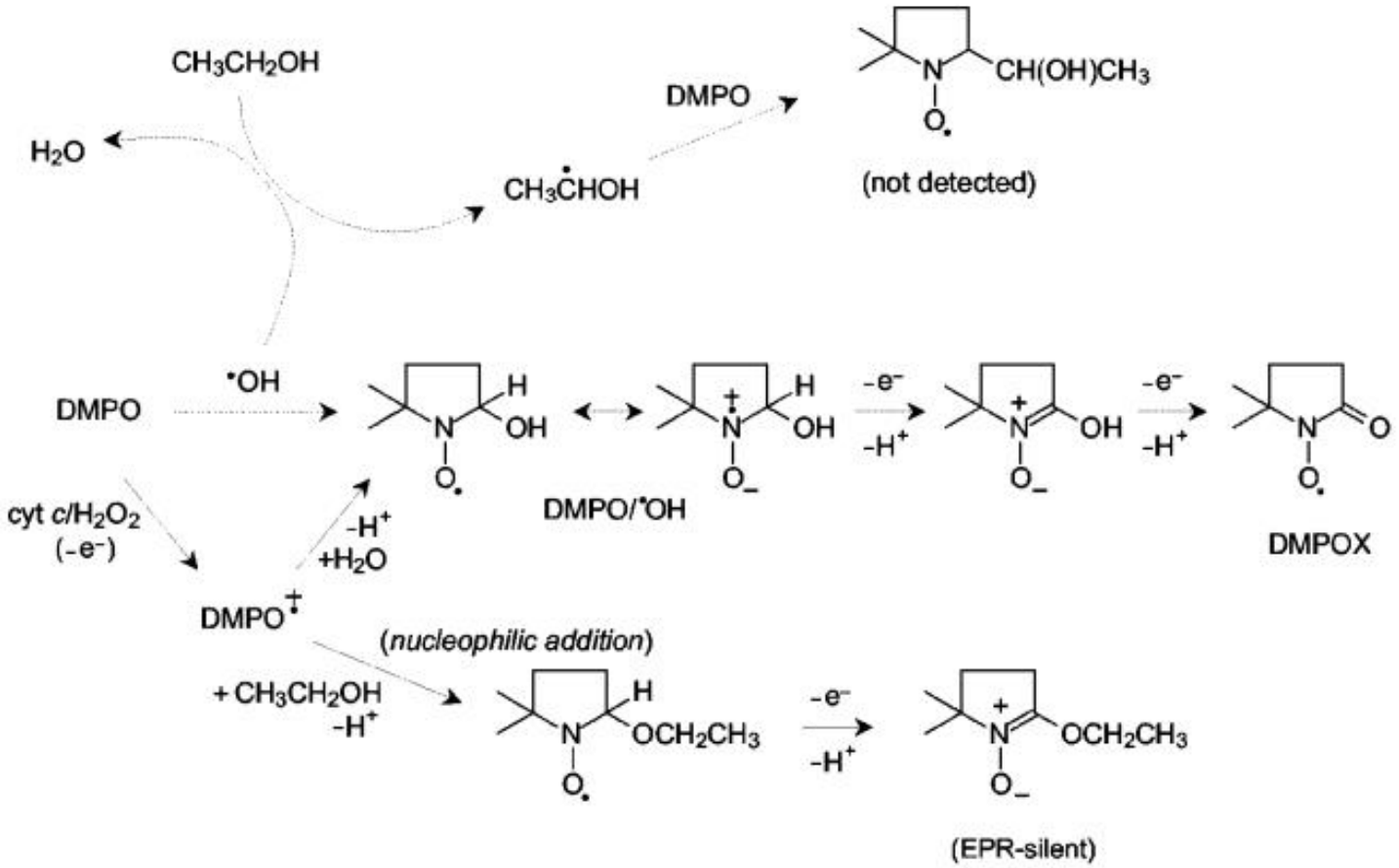

SCHEME 1. **Proposed mechanism for the generation of DMPOX from DMPO by cyt *c*/H_2O_2 and its suppression by ethanol.** DMPOX is the 2-electron oxidation product of the DMPO/hydroxyl radical adduct (DMPO/˙OH). As the α-hydroxyethyl radical adduct was not detected upon the inclusion of ethanol, formation of the DMPO/˙OH adduct cannot involve the trapping of free ˙OH (*dashed arrows*). Instead, it is proposed that DMPO/˙OH is formed by inverted spin trapping, involving the nucleophilic addition of water to the DMPO radical cation, formed by 1-electron oxidation of the spin trap by cyt *c*/H_2O_2 (which is also responsible for further oxidation of DMPO/˙OH to DMPOX). Ethanol is proposed to inhibit the formation of DMPOX by competing with water for nucleophilic addition to the DMPO radical cation, eventually forming an EPR-silent nitrone.

Andrew L., *et al.*, *JBC*, **2003**, *278*, 29410

Effects of PDT on HT-29 cells

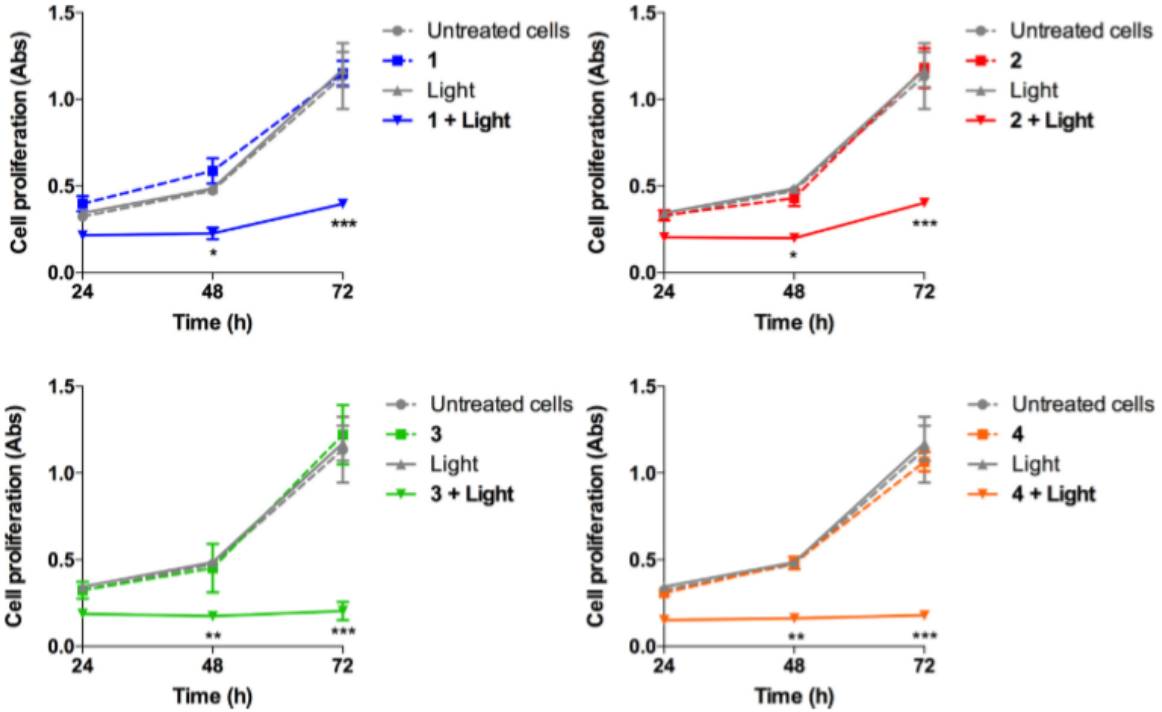

Fig. 7. Effects of photodynamic treatment on HT-29 cell growth. HT-29 cells were incubated for 24 h with the various porphyrins (1, 2 and 4 at 500 μM; 3 at 250 μM) and then exposed to light power at 51.8 mW/cm² for 5 min at 400–1050 nm. Cell proliferation was evaluated after 24, 48 and 72 h using the WST-1 assay. Statistically significant difference *versus* untreated cells: * $p < 0.05$, ** $p < 0.01$, *** $p < 0.001$.

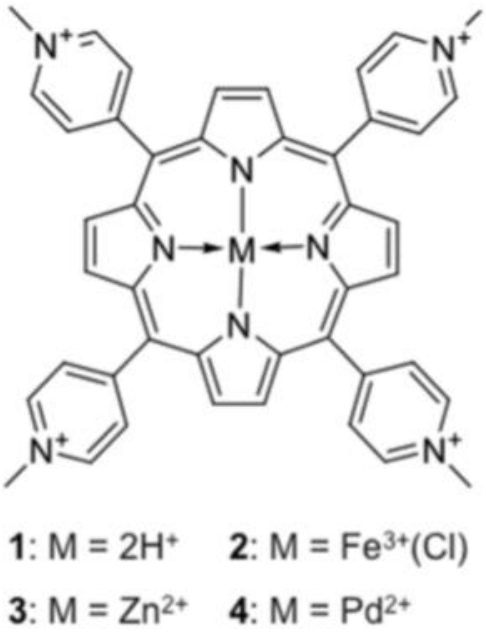

Fig. 1. Structures of porphyrins 1–4.

- All porphyrins induced a significant reduction in cell proliferation under light irradiation.

F. Giuntini, *et al., Free Radical Biology and Medicine,* **2018**, *121*, 190

ROS production after SDT

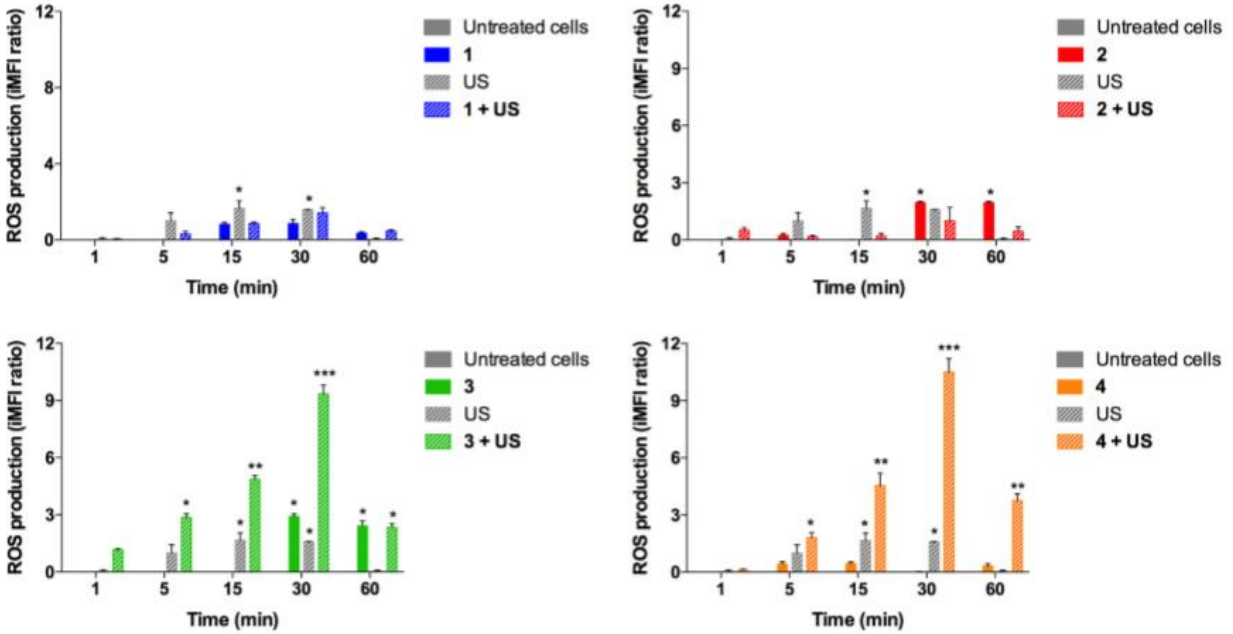

Fig. 8. HT-29 reactive oxygen species production after sonodynamic treatment. HT-29 cells were exposed to US (1.5 W/cm^2 for 5 min at 1.866 MHz) either alone or after 24 h incubation with the various porphyrins (**1**, **2** and **4** at 500 μM; **3** at 250 μM). ROS levels were determined according to the 2',7'-dichlorofluorescein diacetate (DCF-DA) assay using flow cytometry and expressed as the integrated average fluorescence ratio (iMFI) ratio, as described in Materials and Methods. Statistically significant difference *versus* untreated cells (represented by a dashed lines): * $p < 0.05$, ** $p < 0.01$, *** $p < 0.001$.

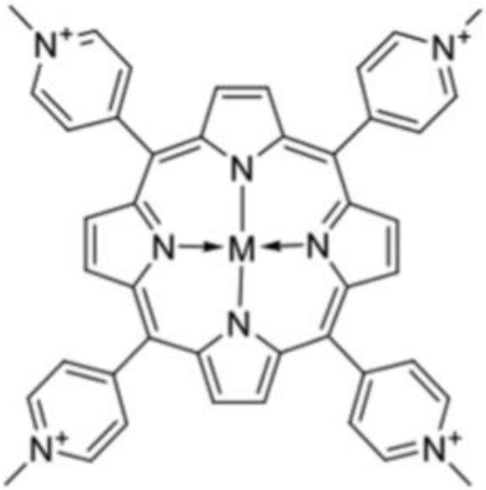

Fig. 1. Structures of porphyrins **1**–**4**.

- Porphyrin 3 and 4 showed ROS emission after US irradiation.
- Porphyrin 4 showed the highest US-responsiveness.

F. Giuntini, *et al., Free Radical Biology and Medicine,* **2018**, *121*, 190

ROS production after PDT

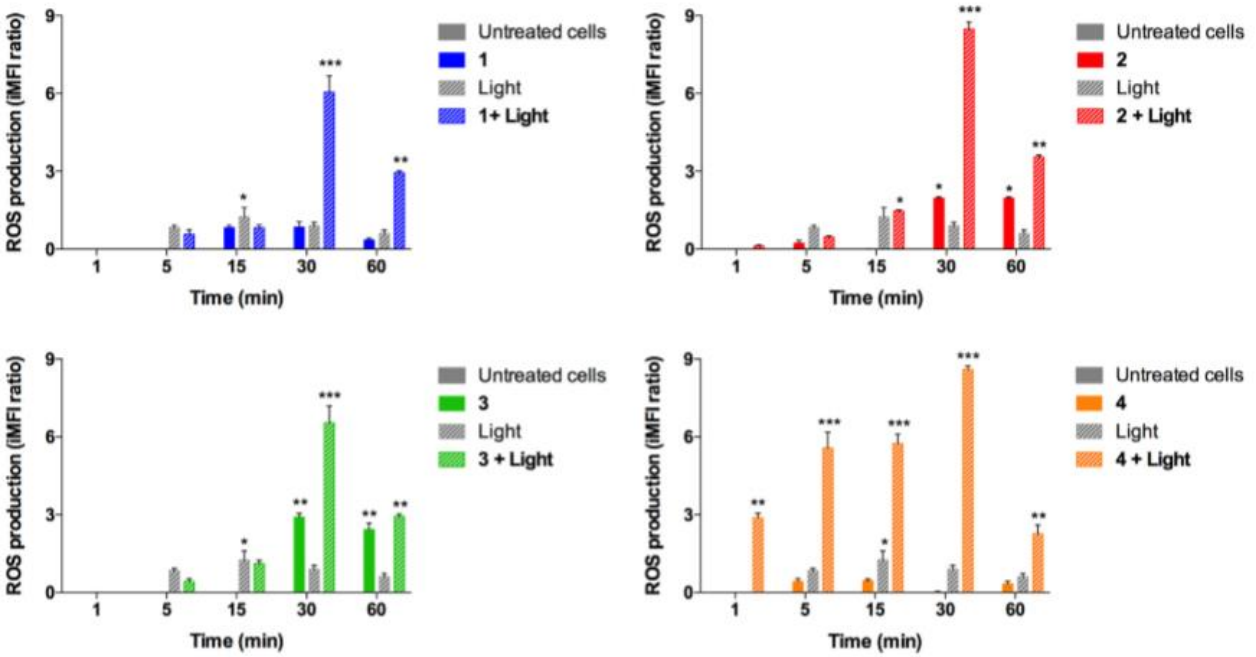

Fig. 9. HT-29 reactive oxygen species production after photodynamic treatment. HT-29 cells were exposed to light (51.8 mW/cm^2 for 5 min at 400–1050 nm), either alone or after cell incubation for 24 h with the various porphyrins (**1**, **2** and **4** at 500 μM; **3** at 250 μM). ROS levels were determined according to the 2',7'-dichlorofluorescein diacetate (DCF-DA) assay using flow cytometry and expressed as the integrated average fluorescence ratio (iMFI) ratio, as described in Materials and Methods. Statistically significant difference *versus* untreated cells (represented by a dashed lines): * $p < 0.05$, ** $p < 0.01$, *** $p < 0.001$.

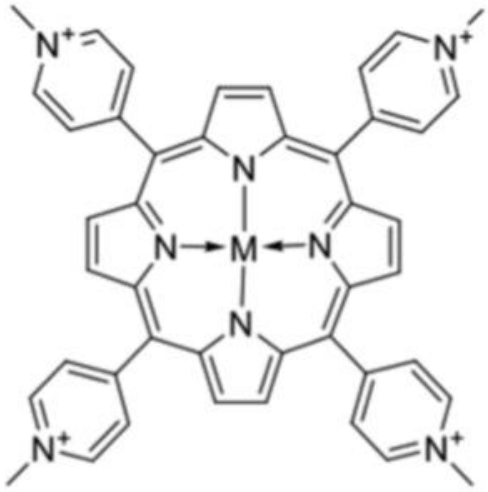

Fig. 1. Structures of porphyrins **1**–**4**.

- Every porphyrin produced more ROS after light irradiation than after US irradiation.
- Porphyrin 4 showed the most ROS emission.

F. Giuntini, *et al., Free Radical Biology and Medicine,* **2018**, *121*, 190

Cell death analysis

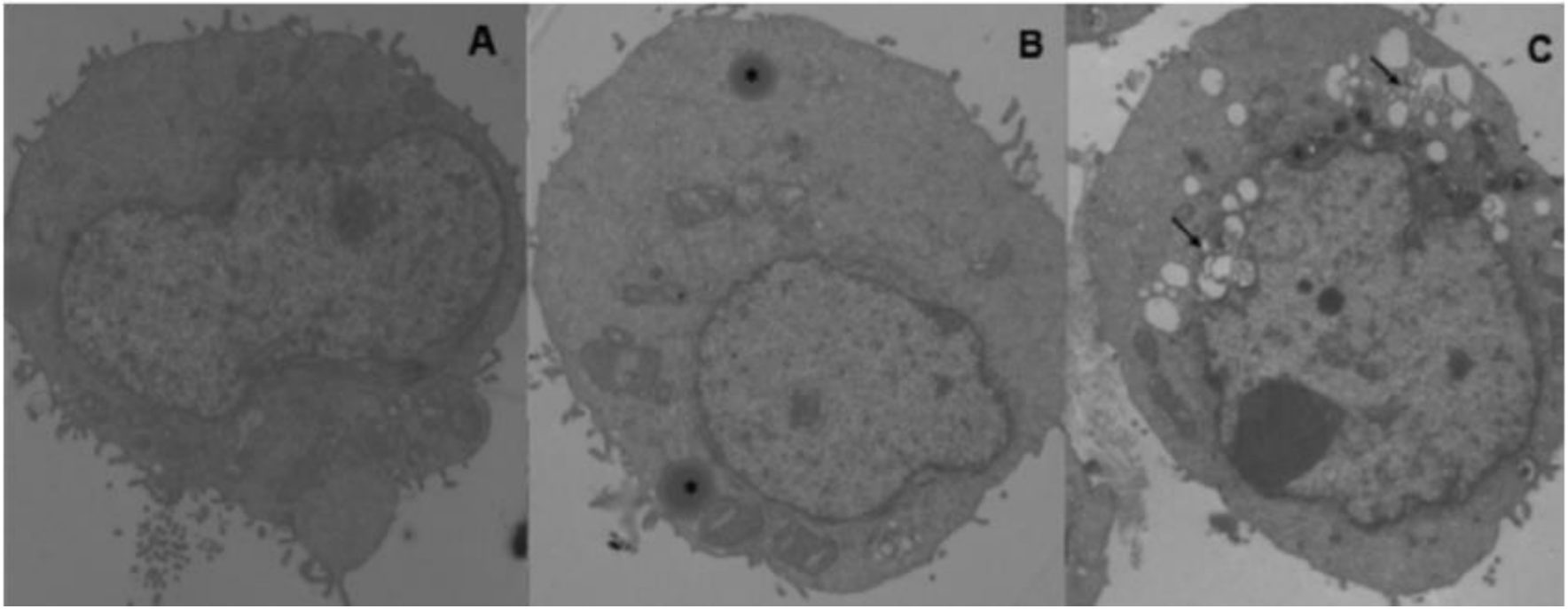

Fig. 10. Representative TEM images of HT-29 cells after sonodynamic treatment with porphyrin **4**. Untreated cells (A, 7500x), cells only exposed to US (1.5 W/cm^2 for 5 min at 1.866 MHz; B, 7500x) and cells 12 h after sonodynamic treatment with porhyrin **4** having been pre-incubated for 24 h at 500 μM (C, 6000x; D, 12,000x) are displayed. Vesicles that contained residual digested material or cellular content are indicated by arrows and lipid droplets by stars.

Antibody-drug conjugate (ADC)

- 2 types of Drug moiety

- For PDT, SDT
- Don’t have to release the Drug moieties.

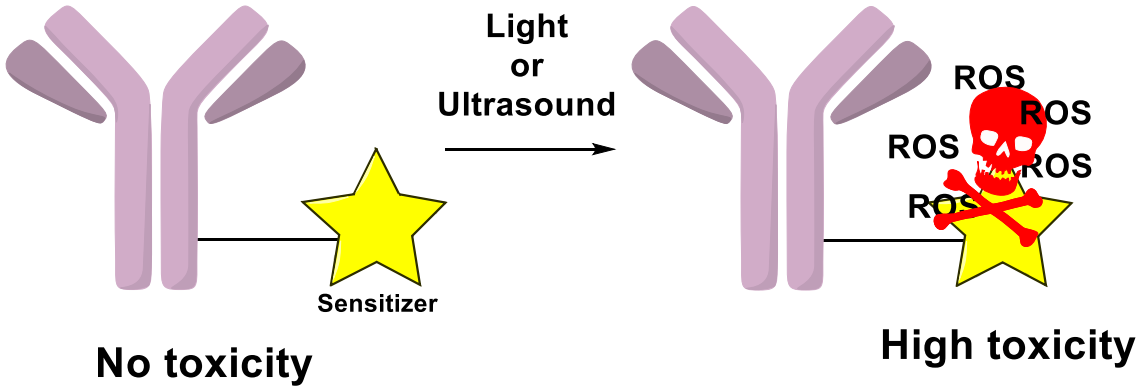

- Common case
- Need to release the Drug moieties.

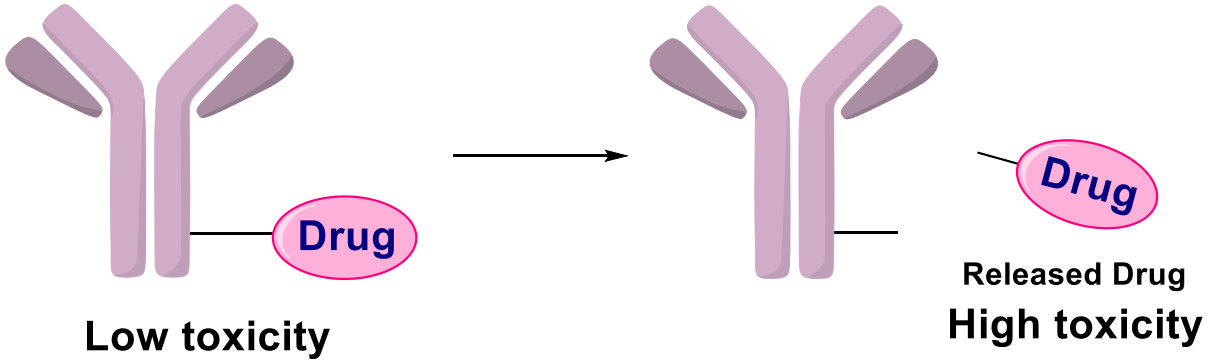

Enzyme & Photo cleavable linker

- Enzyme-cleavable linker

  Jessica R. M., *et al.*,

  The AAPS Journal, **2015**, *17*, 339

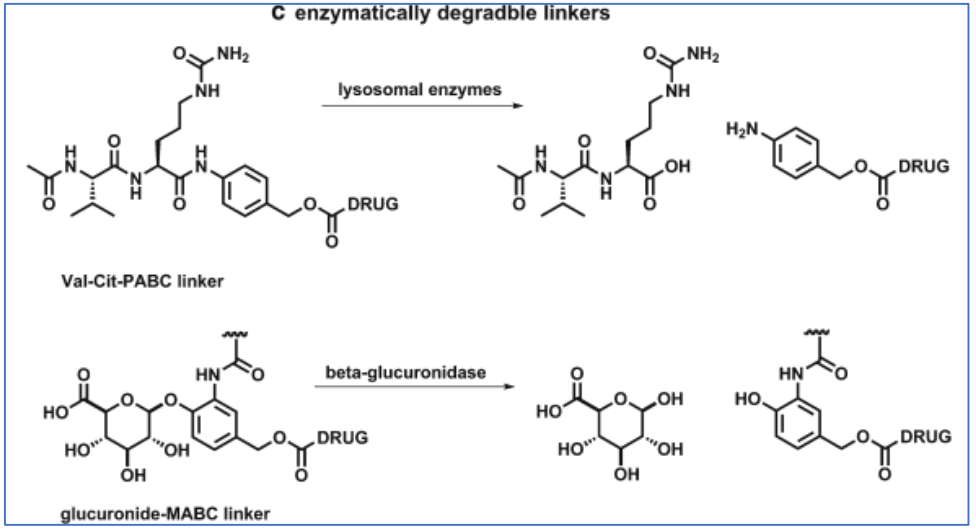

- Photo-cleavable linker

  Roger R. N., *et al.*,

  ACS Cent. Sci., **2017**, *3*, 329

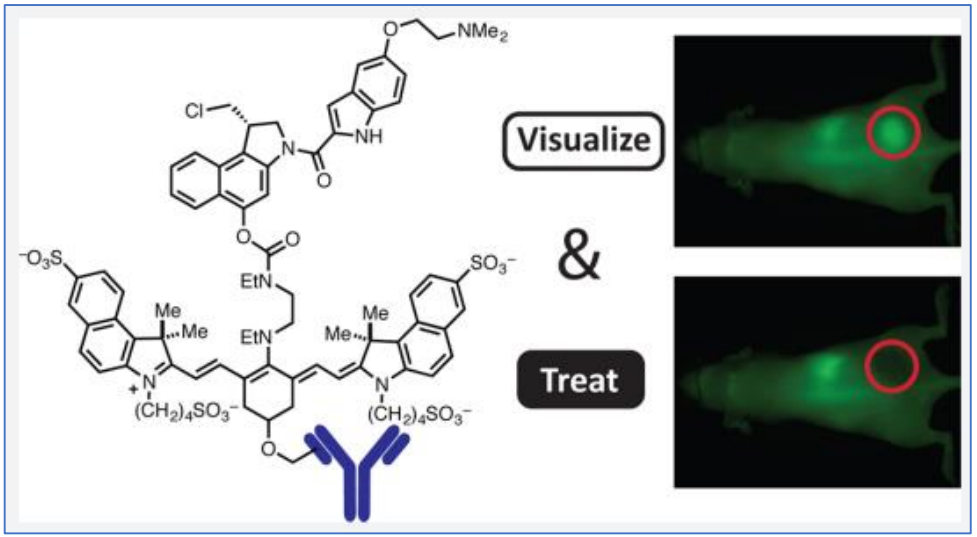

Sonolysis linker

- Sonolysis

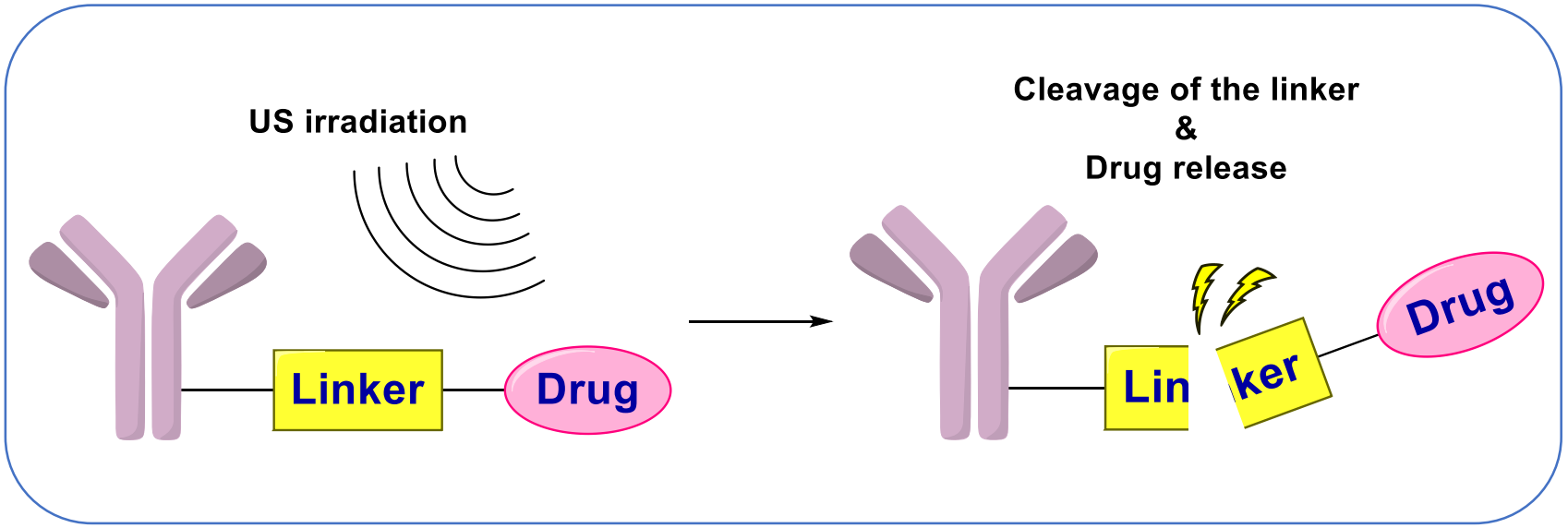

- Sonolysis linker will realize non-invasive treatment of tumors in the deeper place of the body.

Example of sonolysis reaction

- Sonolysis

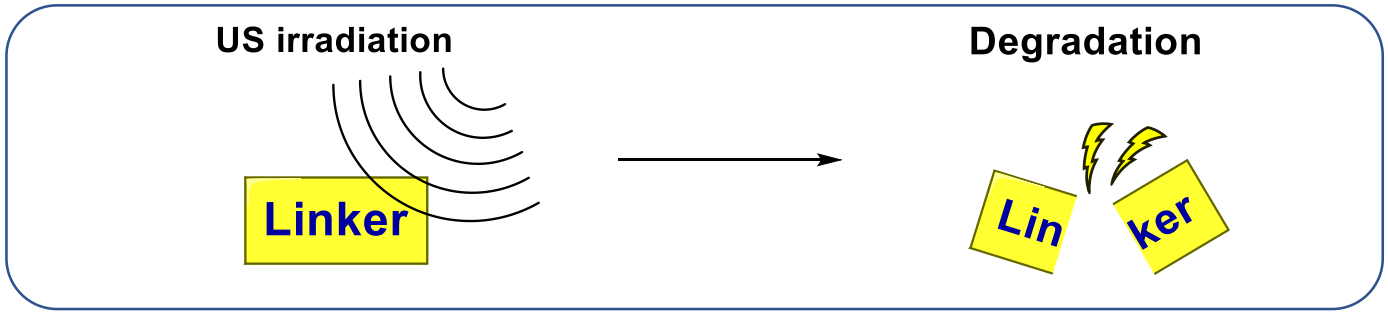

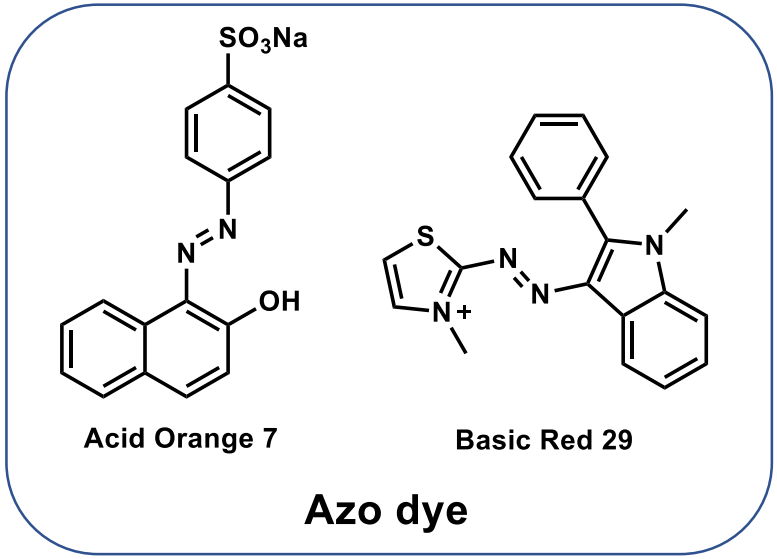

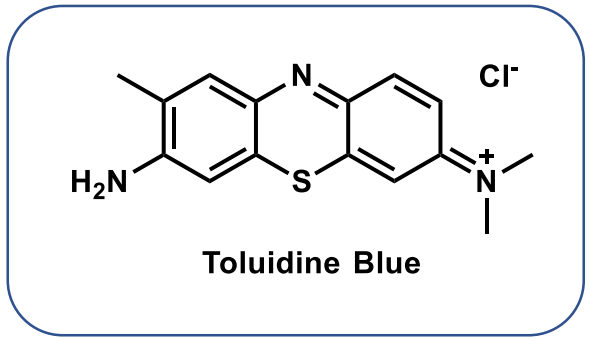

etc...

Kenneth S. S., *et al.*, *Annu. Rev. Phys. Chem.*, **2008**, *59*, 659

Zineb B., *et al., Turk. J. Chem.*, **2017**, *41*, 99

N.E. Chadi, *et al., Sep. Purif. Technol.*, **2018**, *200*, 68

Degradation of NBB by US in water

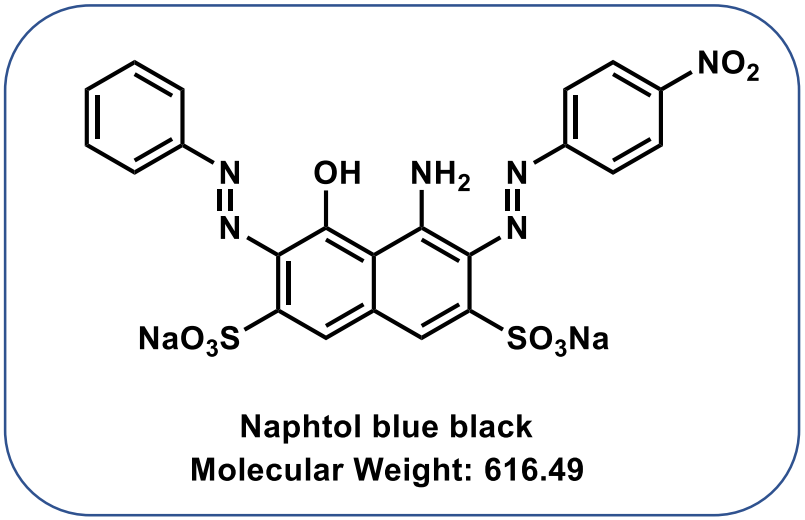

Naphtol blue black
Molecular Weight: 616.49

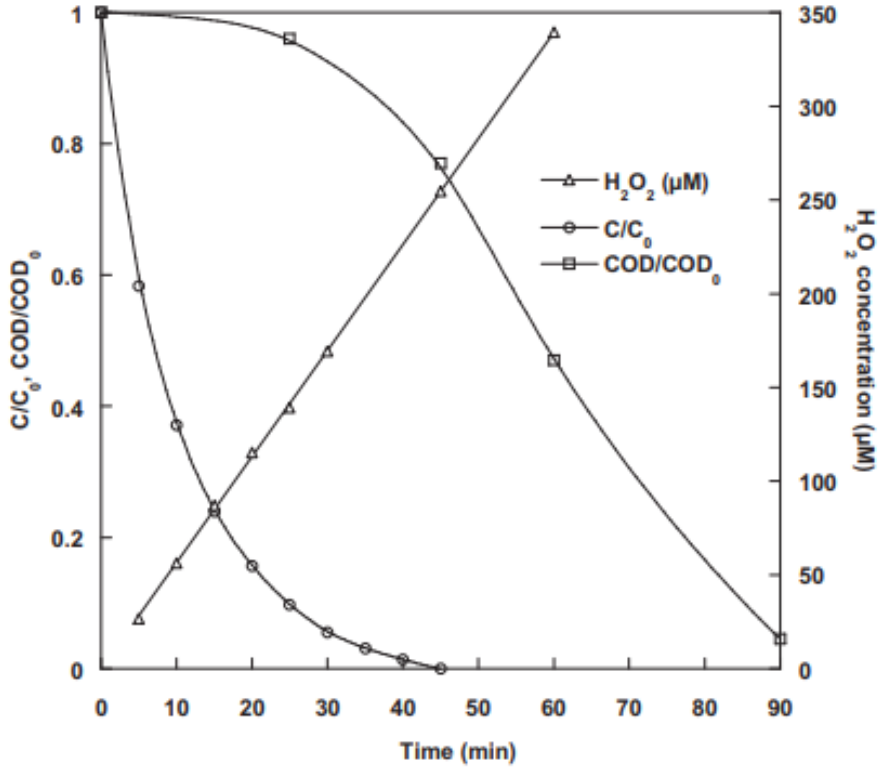

Fig. 2. Kinetics of NBB elimination, COD abatement and H_2O_2 evolution (in pure water) during ultrasonic treatment of an aerated solution of NBB (conditions: volume: 300 mL, initial dye concentration: 5 mg L^{-1}, temperature: 25 °C, pH ~ 6, frequency: 585 kHz, acoustic intensity: 3.58 W cm^{-2}).

- The NBB concentration decreased exponentially with time.
- In absence of substrate, the concentration of H_2O_2 increased linearly with sonication time.

H. Ferkous, *et al.*, *Ultrasonics Sonochemistry*, **2015**, *26*, 40

Sonolysis by safe ultrasound

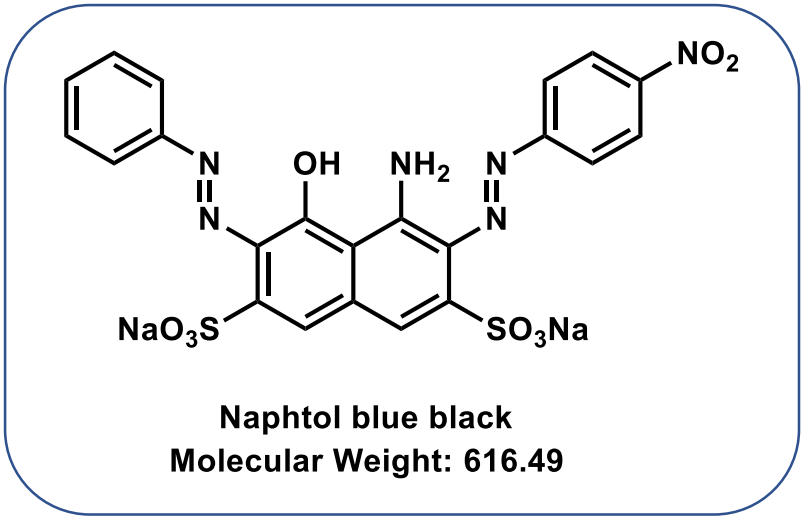

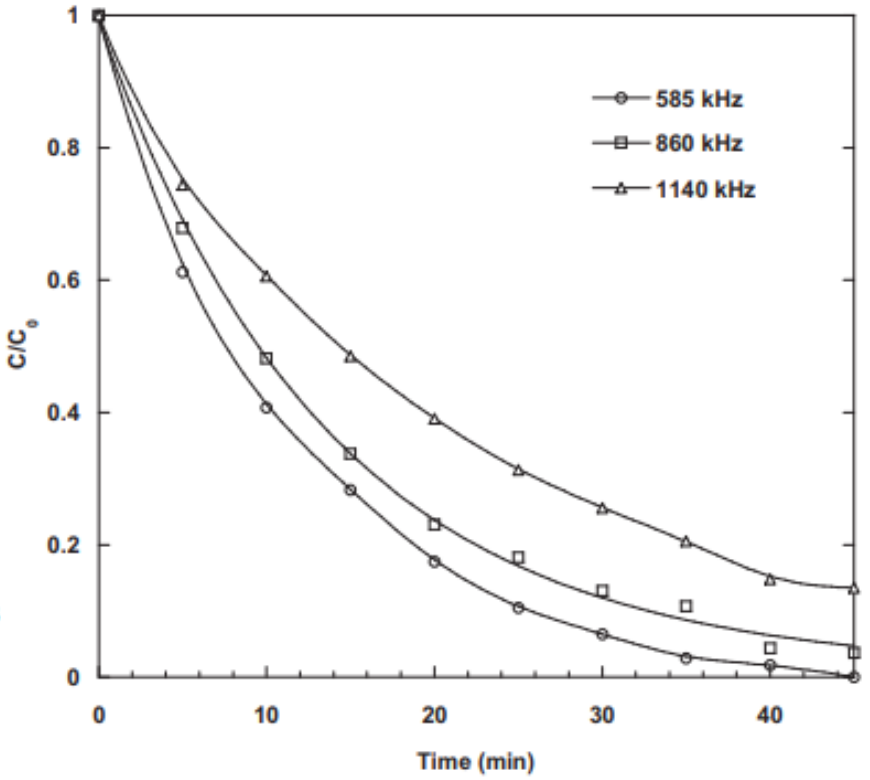

Fig. 6. Effect of ultrasonic frequency on the sonochemical degradation of NBB (conditions: volume: 300 mL, initial dye concentration: 5 mg L^{-1}, temperature: 25 °C, pH ~ 6, frequency: 585–1140 kHz, acoustic intensity: 3.58 W cm^{-2}).

H. Ferkous, *et al.*, *Ultrasonics Sonochemistry*, **2015**, *26*, 40

Sonolysis by safe ultrasound

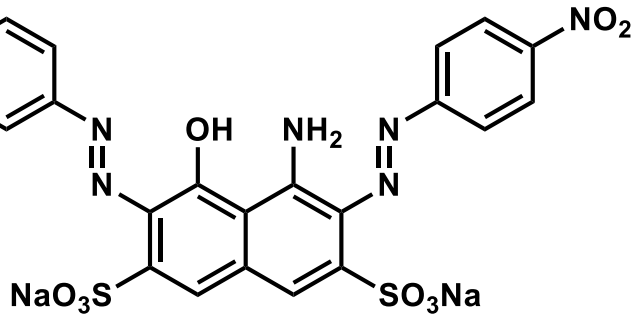

Naphtol blue black
Molecular Weight: 616.49

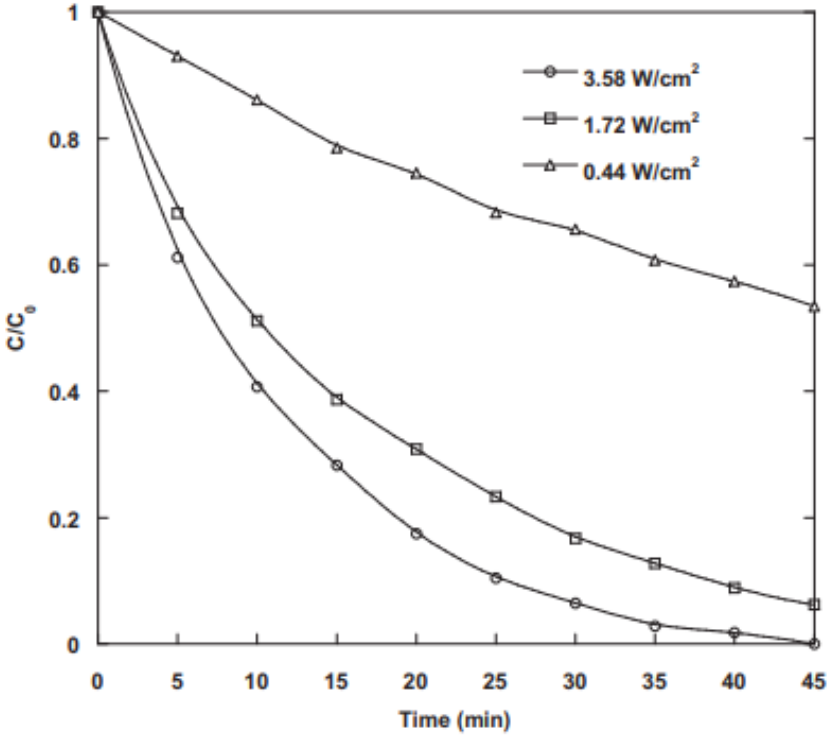

Fig. 5. Effect of acoustic intensity on the sonochemical degradation of NBB (conditions: volume: 300 mL, initial dye concentration: 5 mg L^{-1}, temperature: 25 °C, pH ~ 6, frequency: 585 kHz, acoustic intensity: 0.44–3.58 W cm^{-2}).

H. Ferkous, *et al.*, *Ultrasonics Sonochemistry*, **2015**, *26*, 40

N_2 inhibits sonolysis reaction competitively.

- N_2 is reacted in water by US

$$H_2O \xrightarrow{)))} \cdot OH + \cdot H \quad (1)$$

$$\cdot OH + \cdot OH \rightarrow H_2O_2 \quad (2)$$

$$O_2 \xrightarrow{)))} \cdot O\cdot + \cdot O\cdot \quad (3)$$

$$N_2 + \cdot O\cdot \rightarrow \cdot NO + N\cdot \quad (4)$$

$$O_2 + N\cdot \rightarrow \cdot O\cdot + \cdot NO \quad (5)$$

$$\cdot O\cdot + \cdot NO \rightarrow \cdot NO_2 \quad (6)$$

$$\cdot OH + \cdot NO \rightarrow HNO_2 \rightarrow NO_2^- + H^+ \quad (7)$$

$$\cdot NO_2 + \cdot OH \rightarrow HNO_3 \rightarrow NO_3^- + H^+ \quad (8)$$

$$\cdot NO_2 + \cdot NO \rightarrow N_2O_3 \quad (9)$$

$$2\cdot NO_2 \rightarrow N_2O_4 \quad (10)$$

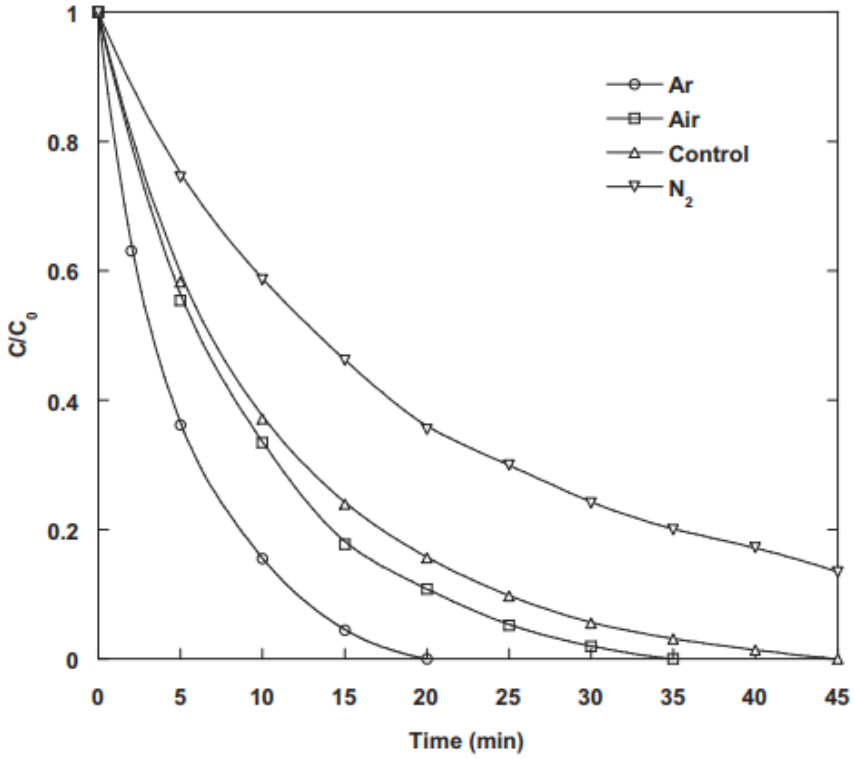

Fig. 7. Effect of different dissolved gases on the sonochemical degradation of NBB (conditions: volume: 300 mL, initial dye concentration: 5 mg L^{-1}, temperature: 25 °C, pH ~ 6, frequency: 585 kHz, acoustic intensity: 3.58 W cm^{-2}).

J. Yao *et al.*, *Ultrason. Sonochem.*, **2018**, *42*, 42

Supeno, *et al., Ultrason. Sonochem.*, **2000**, *7*, 109

- N-N bond is cleavable in water under US exposure.

H_2O_2 evolution (Method)

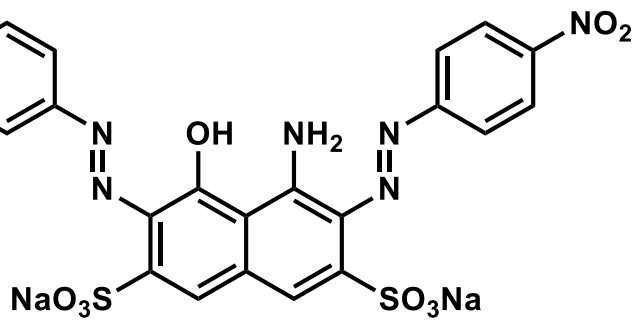

Naphtol blue black
Molecular Weight: 616.49

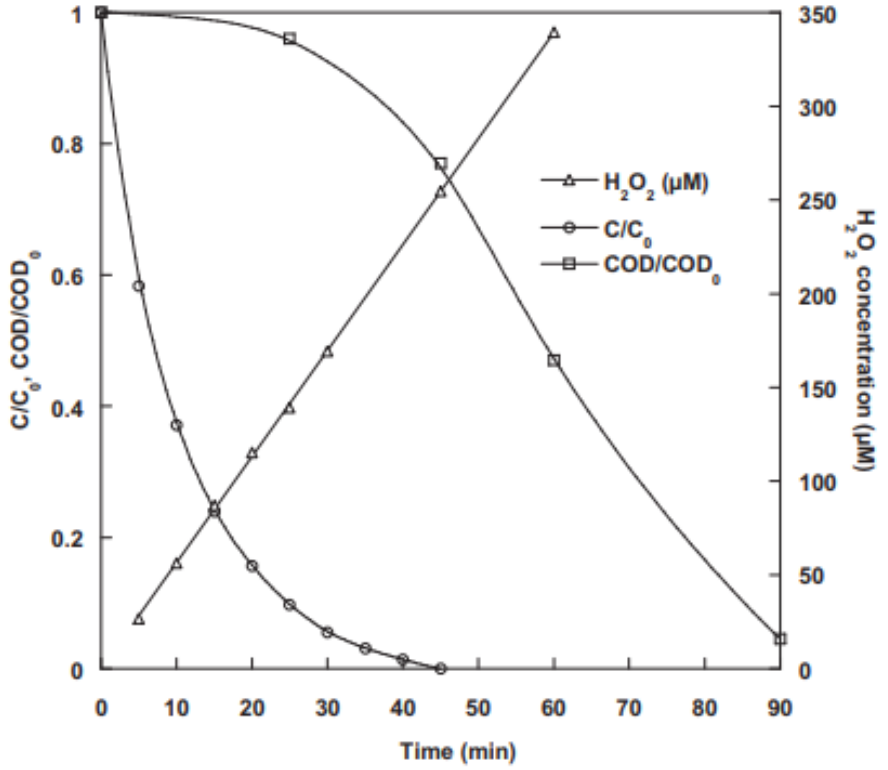

Fig. 2. Kinetics of NBB elimination, COD abatement and H_2O_2 evolution (in pure water) during ultrasonic treatment of an aerated solution of NBB (conditions: volume: 300 mL, initial dye concentration: 5 mg L^{-1}, temperature: 25 °C, pH ~ 6, frequency: 585 kHz, acoustic intensity: 3.58 W cm^{-2}).

1 mL of potassium iodide (0.1 M) and 20 μL of ammonium heptamolybdate (0.01 M). The iodide ion (I^-) reacts with H_2O_2 to form the triiodide ion (I_3^-). The mixed solutions were allowed to stand for 5 min before absorbance was measured. The absorbance was recorded with a UV–visible spectrophotometer (Lightwave II) at the maximum wavelength of the formed triiodide (I_3^-) (352 nm; the molar absorptivity = 26,300 L mol^{-1} cm^{-1}).

H. Ferkous, *et al.*, *Ultrasonics Sonochemistry*, **2015**, *26*, 40

COD abatement (Method)

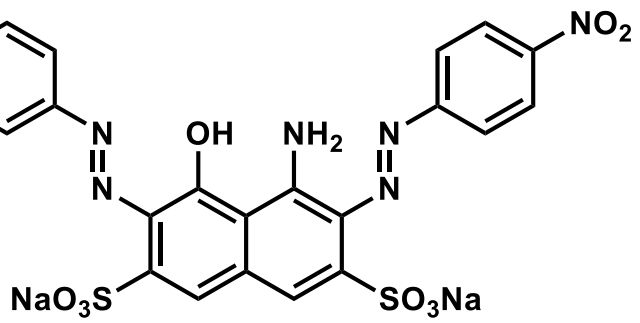

Naphtol blue black
Molecular Weight: 616.49

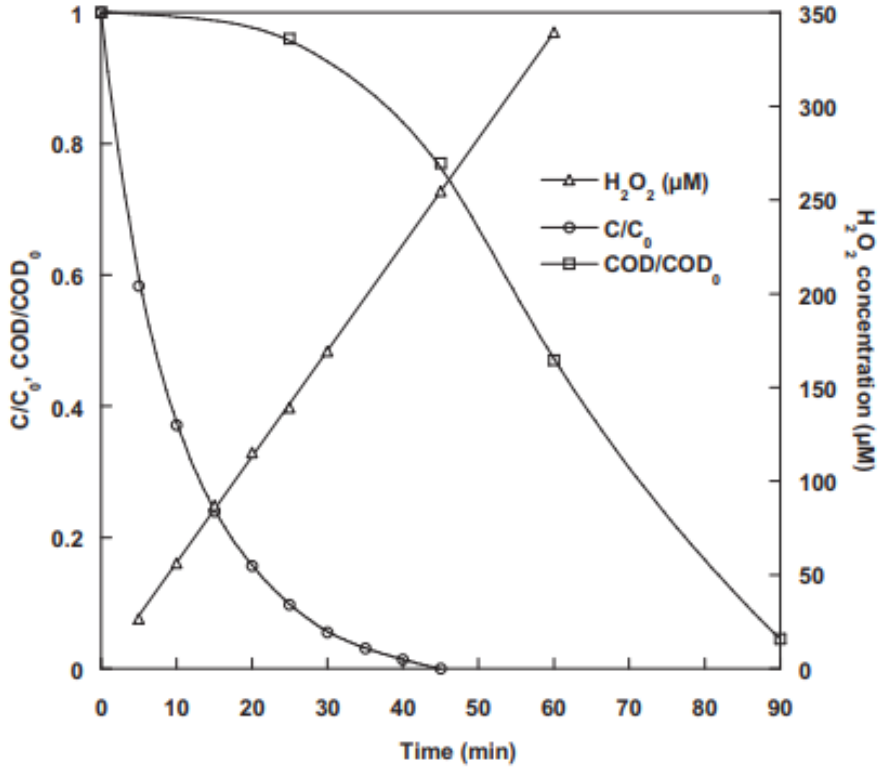

Fig. 2. Kinetics of NBB elimination, COD abatement and H_2O_2 evolution (in pure water) during ultrasonic treatment of an aerated solution of NBB (conditions: volume: 300 mL, initial dye concentration: 5 mg L^{-1}, temperature: 25 °C, pH ~ 6, frequency: 585 kHz, acoustic intensity: 3.58 W cm^{-2}).

COD: Chemical oxygen demand.

Test solution (2 mL) was transferred into the dichromate reagent and digested at 150 ° C for 2 h. The optical density for the color change of dichromate solution was determined with a spectrophotometer at 440 nm.

H. Ferkous, *et al.*, *Ultrasonics Sonochemistry*, **2015**, *26*, 40